Main Manuscript for

The function of juvenile-adult transition axis in female sexual receptivity of *Drosophila melanogaster*

Jing Li[1,2,†,*], Chao Ning[3,4,†], Yaohua Liu[2,5,†], Bowen Deng[6], Bingcai Wang[2,7], Kai Shi[2,7], Rencong Wang[2,7], Ruixin Fang[1] and Chuan Zhou[1,2,7]

[1]*Institute of Molecular Physiology, Shenzhen Bay Laboratory, Shenzhen 518132, China.*
[2]*State Key Laboratory of Integrated Management of Pest Insects and Rodents, Institute of Zoology, Chinese Academy of Sciences, Beijing 100101, China.*
[3]*National Laboratory of Biomacromolecules, New Cornerstone Science Laboratory, CAS Center for Excellence in Biomacromolecules, Institute of Biophysics, Chinese Academy of Sciences, 100101, Beijing, China.*
[4]*CAS Key Laboratory of Genome Sciences and Information, Beijing Institute of Genomics, Chinese Academy of Sciences, Beijing 100101, China.*
[5]*Department of Plant Protection, Shanxi Agricultural University, Jinzhong 30801, China*
[6]*Chinese Institute for Brain Research, Peking-Tsinghua Center for Life Sciences, Zhongguancun Life Sciences Park, Beijing 102206, China.*
[7]*University of Chinese Academy of Sciences, Beijing 100049, China.*
[†]*These authors contributed equally to this work*

---

*Jing Li, Email: lijing@szbl.ac.cn

Author Contributions: Jing Li, Conceptualization, Resources, Data curation, Writing - original draft, review and editing, Funding acquisition; Chao Ning and Yaohua Liu, Data curation; Bowen Deng, Resources; Bingcai Wang, Kai Shi and Rencong Wang, Software; Ruixin Fang, Data curation; Chuan Zhou, Conceptualization, Funding acquisition.

Competing Interest Statement: The authors declare no competing interest.

Impact statement: Prothoracicotropic hormone and ecdysone belonging to the insect PG axis modulate virgin female sexual receptivity.

Funding information: This work was supported by the Institute of Molecular Physiology, Shenzhen Bay Laboratory (NO.21260061 to Chuan Zhou, S239201006 to Jing Li), National Natural Science Foundation of China (NO.Y711241133 to Chuan Zhou) and Strategic Priority Research Program of the Chinese Academy of Sciences (NO.Y929731103 to Chuan Zhou).

Abstract

Female sexual receptivity is essential for reproduction of a species. Neuropeptides play the main role in regulating female receptivity. However, whether neuropeptides regulate female sexual receptivity during the neurodevelopment is unknown. Here we found the peptide hormone prothoracicotropic hormone (PTTH), which belongs to the insect PG axis, negatively regulated virgin female receptivity through ecdysone during neurodevelopment in *Drosophila melanogaster*. We identified PTTH neurons as doublesex-positive neurons, they regulated virgin female receptivity before the metamorphosis during the 3rd-instar larval stage. PTTH deletion resulted in the increased EcR-A expression in the whole newly formed prepupae. Furthermore, the ecdysone receptor EcR-A in pC1 neurons positively regulated virgin female receptivity during metamorphosis. The decreased EcR-A in pC1 neurons induced abnormal morphological development of pC1 neurons without changing neural activity. Among all subtypes of pC1 neurons, the function of EcR-A in pC1b neurons was necessary for virgin female copulation rate. These suggested that the changes of synaptic connections between pC1b and other neurons decreased female copulation rate. Moreover, female receptivity significantly decreased when the expression of PTTH receptor Torso was reduced in pC1 neurons. This suggested that PTTH not only regulates female receptivity through ecdysone but also through affecting female receptivity associated neurons directly. The PG axis has similar functional strategy as the HPG axis in mammals to trigger the juvenile–adult transition. Our work suggests a

general mechanism underlying which the neurodevelopment during maturation regulates female sexual receptivity.

Keywords: prothoracicotropic hormone, *Drosophila*, female sexual receptivity, ecdysone, pC1 neurons

Introduction

The success of copulation is important for the reproduction of a species. *Drosophila melanogaster* provides a powerful system to investigate the neuronal and molecular mechanism of sexual behaviors. Females decide to mate or not according to their physiological status and the environmental condition (Dickson, 2008). Sexually mature adult virgin females validate males after sensing the courtship song and male-specific sex pheromone, receive courtship with pausing and opening the vaginal plate (Ferveur, 2010; Greenspan et al., 2000; Hall, 1994; Wang et al., 2021). If the female is not willing to mate, she may kick her legs, flick her wings, or extrude the ovipositor to deter males (Connolly et al., 1973). Mated females reject males for several days after mating mainly through more ovipositor extrusion and less opening the vaginal plate (Fuyama et al., 1997; Wang et al., 2021). These options need the establishment of neural circuits for female sexual receptivity. However, the associated mechanism of neural maturation and the effect of neural maturation on female sexual receptivity is little known.

88 *doublesex* (*dsx*) and *fruitless* (*fru*) are the terminal genes in sex determination
89 regulatory hierarchy. They specify nearly all aspects of somatic sexual differentiation,
90 including the preparation for sexual behaviors (Dickson, 2008; Manoli et al., 2013;
91 Manoli et al., 2006; Mellert et al., 2012; Pavlou et al., 2013; Siwicki et al., 2009;
92 Yamamoto, 2007; Yamamoto et al., 2013). In males, expression of male-specific Fru^M
93 (Billeter et al., 2006; Demir et al., 2005; Hall, 1978; Manoli et al., 2005; Stockinger et al.,
94 2005) and male-specific Dsx^M (Kohatsu et al., 2011; Pan et al., 2014; Pan et al., 2011;
95 Rideout et al., 2010) are important for male courtship behaviors. In females, although
96 functional Fru protein is not translated, neurons with Dsx^F or *fru* P1 promoter regulate
97 some aspects of the female sexual behaviors (Kvitsiani et al., 2006; Rideout et al.,
98 2010). *Fru and dsx* are involved in regulating the sexual dimorphism during
99 neurodevelopment (Yamamoto et al., 2013). For instance, the sexual dimorphism of P1
100 and mAL neurons which are all associated with male courtship and aggression
101 behaviors (Clowney et al., 2015; Hoopfer et al., 2015; Kimura et al., 2008; Kohatsu et
102 al., 2011; Pan et al., 2012; Sengupta et al., 2022; von Philipsborn et al., 2011) is the
103 result of regulation by Dsx and/or Fru (Ito et al., 2012; Kimura et al., 2008). In the cis-
104 vaccenyl acetate (cVA) pathway, which induces the courtship inhibiting in males
105 (Kurtovic et al., 2007; Wang et al., 2010), the first-order to the fourth-order components
106 are all fru-Gal4-positive neurons and are either male-specific or sexually dimorphic
107 (Ruta et al., 2010). However, the role of Dsx^F in neurodevelopment associated with
108 female sexual behaviors is little understood.
109

110 During postembryonic development, the PG axis triggers the juvenile–adult transition,
111 similar to the function of hypothalamic–pituitary–gonadal (HPG) axis in mammals
112 (Herbison, 2016; Pan et al., 2019). Hormones of the PG axis act to transform the larval
113 nervous system into an adult version (Truman et al., 2023). Ecdysone belonging to the
114 PG axis is the prime mover of insect molting and metamorphosis and is involved in all
115 phases of neurodevelopment, including neurogenesis, pruning, arbor outgrowth, and
116 cell death (Truman et al., 2023). The neurons read the ecdysteroid titer through two
117 isoforms of the ecdysone receptor, EcR-A and EcR-B1, according to spatial and
118 temporal conditions in the central nervous system (Riddiford et al., 2000; Truman et al.,
119 1994). EcR-A is required in fru P1-expressing neurons for the establishment of male-
120 specific neuronal architecture, and ecdysone receptor deficient males display increased
121 male–male courtship behavior (Dalton et al., 2009; Ganter et al., 2007). However, how
122 ecdysone regulates the neurodevelopment associated with female sexual receptivity,
123 especially the fru^+ and dsx^+ neurons, is unknown.
124
125 Much of studies to understand female sexual receptivity has focused on its regulation.
126 How a female respond to males is highly dependent on whether or not she has
127 previously mated. In virgin females, dsx^+ pCd neurons respond to the cVA, while dsx^+
128 pC1 neurons also respond to male courtship song (Zhou et al., 2014). The receptive
129 females open the vaginal plate (VPO) through activation of the dsx^+ vpoDN neurons
130 (Wang et al., 2021). After mated, sex peptide in the seminal fluid binds to the fru^+ dsx^+
131 sex peptide sensory neurons (SPSNs) in the female uterus. Then neuronal activity in
132 the dsx^+ sex peptide abdominal ganglion (SAG) neurons of the ventral nerve cord and in

133 the pC1 neurons is reduced (Avila et al., 2011; Feng et al., 2014; Häsemeyer et al.,
134 2009; Kubli, 2003; Wang et al., 2020b; Yang et al., 2009; Zhou et al., 2014). Therefore,
135 the sexual receptivity is reduced with less VPO and more ovipositor extrusion (OE)
136 which is controlled by dsx$^+$ DpN13 neurons (Wang et al., 2020a). In addition,
137 neuropeptides and monoamines play a critical role in regulation of the female
138 receptivity. The neuropeptides Drosulfakinin, myoinhibitory peptides and SIFamide are
139 involved in female sexual receptivity (Jang et al., 2017; Terhzaz et al., 2007; Wang et
140 al., 2022). As monoamines, dopamine, serotonin and octopamine are pivotal to female
141 sexual behaviors (Ishimoto et al., 2020; Ma et al., 2022; Neckameyer, 1998; Rezával et
142 al., 2014). So far, the identified neuropeptides and monoamines modulating female
143 sexual receptivity all function during the adult stage. However, whether neuropeptides
144 or monoamines regulate the establishment of neural circuits for female sexual
145 receptivity is unknown.
146
147 To explore the factors that regulate *Drosophila* virgin female receptivity especially
148 during neurodevelopment, we did a knock-out screen including most of CCT members.
149 We discovered a requirement for the prothoracicotropic hormone (PTTH) during
150 postembryonic development for virgin female receptivity. We also found that PTTH
151 neurons expressing PTTH are dsx$^+$ neurons. PTTH, a brain derived neuropeptide
152 hormone, is the primary promoter of the synthesis of steroid hormone 20-
153 hydroxyecdysone (20E) (McBrayer et al., 2007; Rewitz et al., 2009). Indeed, the
154 enhanced virgin female receptivity due to the loss of PTTH could be rescued through
155 feeding 20E to the 3rd-instar larvae. Because 20E acts through its receptor EcR

156 (Riddiford et al., 2000), we then tested the function of EcR in pC1 neurons which
157 encode the mating status of females (Zhou et al., 2014). The reduced EcR-A expression
158 in pC1 neurons resulted in the abnormal anatomical pattern of pC1 neurons and the
159 reduced female copulation rate. This may be explained by the increased EcR-A in newly
160 formed prepupae resulted from the PTTH deletion. Furthermore, the decreased female
161 copulation rate was due to the reduced EcR-A in pC1b neurons. Besides, we detected
162 the inhibited female receptivity when PTTH receptor torso was decreased in pC1
163 neurons, suggested the direct function of PTTH on other dsx^+ neurons to regulate
164 female receptivity. Thus, in addition to demonstrating the function of PTTH in virgin
165 female receptivity during neurodevelopment, our study identified the necessary role of
166 the normal pC1b neural morphology in virgin female receptivity.
167
168 **Results**
169
170 **PTTH modulates virgin female receptivity**
171
172 In *Drosophila*, neuropeptides and monoamines, belonging to the chemoconnectome
173 (CCT, the entire set of neurotransmitters, neuromodulators, neuropeptides, and their
174 receptors underlying chemotransmission) (Deng et al., 2019), play a critical role in
175 regulation of the female receptivity. To explore the factors that regulate virgin female
176 receptivity especially during neurodevelopment, we screened 108 chemoconnectome
177 (CCT) knock-out lines generated by the CRISPR-Cas9 system (Deng et al., 2019)
178 (unpublished data). The result showed that prothoracicotropic hormone (PTTH) might

179 regulate virgin female receptivity. The deletion mutant *Ptth*^{Delete} removed part of the 5'
180 UTR and almost all coding sequence and is a protein null (**Figure 1A**). We confirmed
181 the PTTH knock-out flies by using PCR analysis at the PTTH locus in genomic DNA
182 samples (**Figure 1B**), by using RT-PCR to identify the loss of PTTH transcripts in cDNA
183 samples (**Figure 1C**) and by detecting the immunoreactivity of PTTH in the central brain
184 (**Figure 1—figure supplement 1A**). Primers used are listed in **Supplementary File 1**.
185 PTTH immunoreactivity was found in the brain of wild-type and heterozygous flies
186 (**Figure 1—figure supplement 1A1 and 1A3**), but was absent in homozygous *Ptth*^{Delete}
187 flies (**Figure 1—figure supplement 1A2**). As the previous study, the *Ptth*^{Delete} larvae
188 lacking PTTH undergo metamorphosis with about 1 day delay compared with the wild
189 type control (Shimell et al., 2018) (data not shown). Besides, the *Ptth*^{Delete} adult male
190 and female flies had the significant increased weight than wild type flies (**Figure 1—**
191 **figure supplement 1B**). This is also consistent with that PTTH regulates developmental
192 timing and body size in *Drosophila* (Mcbrayer et al., 2007; Shimell et al., 2018).
193
194 To confirm the function of PTTH, we tested virgin female receptivity of *Ptth*^{Delete} female
195 flies. We found that the virgin female losing PTTH had significantly higher copulation
196 rate and shorter latency to copulation than wild type flies (**Figure 1D-G**). In addition, the
197 *Ptth*^{Delete} flies had higher copulation rate and lower latency to copulation compared to
198 heterozygous null mutant females within 2 days (**Figure 1D-E**) and within 3 days,
199 respectively (**Figure 1D-F**). The enhanced virgin female receptivity had no relationship
200 either with the attractivity or with the locomotion activity of virgin females (**Figure 1—**
201 **figure supplement 1C-E**). These results suggested that PTTH deletion regulates virgin

202 female receptivity in a dose-dependent manner. Female receptivity increases with the
203 increase of age after eclosion, not only for wild type flies but also PTTH mutants. At the
204 first day after eclosion (**Figure 1D**), maybe the loss of PTTH in *PTTH*^{Delete}/+ flies is not
205 enough for sexual precocity as *PTTH*^{Delete}/*PTTH*^{Delete}. At the second day after eclosion
206 and after (**Figure 1E-G**), the loss of PTTH in *PTTH*^{Delete}/+ flies is enough for sexual
207 precocity compared with wild type flies. However, After the 2nd day of adult, female
208 receptivity of all genotype flies increases sharply. At the 3rd day of adult and after,
209 female receptivity of *PTTH*^{Delete}/*PTTH*^{Delete} reaches the peak and the receptivity of
210 *PTTH*^{Delete}/+ reaches more nearly to *PTTH*^{Delete}/*PTTH*^{Delete} when flies get older (**Figure**
211 **1F-G**). However, the overexpression through PTTH-Gal4>UAS-PTTH is also not
212 sufficient to change female receptivity (**Figure 1—figure supplement 2A**). Similarly,
213 decreased expression of PTTH through PTTH-Gal4>UAS-PTTH-RNAi or dsx-
214 Gal4>UAS-PTTH-RNAi did not result in the similar phenotype to that of
215 *PTTH*^{Delete}/*PTTH*^{Delete} (**Figure 1—figure supplement 2B-C**). It is possible that both
216 decreasing and increasing PTTH expression are not sufficient to change female
217 receptivity.
218
219 Furthermore, we carried out genetic rescue experiments to further confirm the function
220 of PTTH in modulating virgin female receptivity. We used the pan-neuronal driver elav-
221 Gal4 to drive UAS-PTTH expression in PTTH mutant background, although elav-Gal4
222 did not express in PTTH neurons (**Figure 1—figure supplement 2D**). We detected the
223 PTTH signals using PTTH antibody in the rescued female brains (**Figure 1—figure**
224 **supplement 1A4**). We found that neuron-specific expression of PTTH could restore

225 the enhanced copulation rate and shorter latency to copulation in *PTTH*^{Delete}/*PTTH*^{Delete}
226 virgin females (**Figure 1H**). Except for the projection of axons to PG gland, PTTH also
227 carries endocrine function to regulate light avoidance of larvae (Yamanaka et al., 2013).
228 The overexpressed PTTH in other neurons through elav-Gal4>UAS-PTTH may act on
229 the PG gland through endocrine function and then induce the ecdysone synthesis and
230 release. In summary, these results suggested that PTTH regulates virgin female
231 receptivity through ecdysone.
232
233 **Dsx^{+} PTTH neurons regulate virgin female receptivity.**
234 We used new Ptth-Gal4 and Ptth-LexA which inserts Gal4 or LexA sequence before the
235 stop codon of the *Ptth* gene (Deng et al., 2019) to label and manipulate PTTH neurons
236 expressing PTTH. The labeled neurons were the same as reported before (McBrayer et
237 al., 2007; Yamanaka et al., 2013), a pair of bilateral neurosecretory cells in the brain
238 directly innervating the prothoracic gland during the larval stage (**Figure 2A and Figure**
239 **2—figure supplement 1A**). The newly emerged flies had the similar anatomical pattern
240 with that of the larval stage (**Figure 2B and Figure 2—figure supplement 1B**).
241 However, while the prothoracic gland cells are gradually degenerating during pharate
242 adult development (Dai et al., 1991; Roy et al., 2018), the pattern of PTTH neurons
243 labeled by Ptth-Gal4 > UAS-mCD8GFP gradually could not be found before the 10th
244 hour after eclosion (**Figure 2—figure supplement 2**).
245
246 Most identified neurons associated with female sexual behaviors express *doublesex*
247 gene. We asked whether PTTH neurons are a part of the doublesex circuitry or not.

248 Double labeling of dsx-LexA and Ptth-Gal4 neurons (LexAop-tomato,UAS-stinger-
249 GFP/Ptth-LexA;dsx-Gal4/+) revealed that PTTH neurons are all doublesex-positive
250 (**Figure 2C**). We then used an intersectional strategy to visualize overlapped expression
251 between dsx-LexA and Ptth-Gal4 (*UAS > stop > myrGFP/+;LexAop2-FlpL,dsx-*
252 *LexA/Ptth-Gal4*). We observed all PTTH neurons with GFP signals (**Figure 2D**). These
253 results suggested that PTTH neurons are dsx^+ neurons. Furthermore, we wanted to
254 know whether Dsx^F regulates female receptivity in PTTH neurons. We decreased the
255 Dsx^F expression in PTTH neurons and did not detect significantly changed female
256 receptivity (**Figure 2—figure supplement 1C**). We supposed that PTTH neurons have
257 some relationship with other Dsx^F-positive neurons which regulate female receptivity.
258
259 We then analyzed whether PTTH neurons are involved in the modulation of virgin
260 female receptivity. First, we activated PTTH neurons transiently in adult virgin females
261 by driving the temperature-sensitive activator dTrpA1 (Hamada et al., 2008) using Ptth-
262 Gal4. PTTH neurons were activated at 29°C compared with the control treatment at
263 23°C. No significantly different copulation rate or latency to copulation was detected
264 (**Figure 2—figure supplement 3A-C**). This suggested that PTTH neurons do not
265 regulate virgin female receptivity during the adult stage.
266
267 To identify the detail time for the function of PTTH neurons in virgin female receptivity,
268 we inactivated PTTH neurons through kir2.1 under the control of the temporal and
269 regional gene expression targeting system (McGuire et al., 2004). When the experiment
270 was done at the pupal stage is the only situation when the controls were both different

271 from the experimental. (**Figure 2—figure supplement 1D**). However, when PTTH
272 neurons were inactivated during whole pupal or whole adult stages, virgin female
273 copulation rate did not change significantly (**Figure 2—figure supplement 1D**).
274 Furthermore, we activated PTTH neurons at different stages overlapping the
275 postembryonic larval developmental time using dTrpA1 (**Figure 3A**). Stage 1 was from
276 the 1st-instar larvae to six hours before the 3rd-instar larvae. Stage 2 was from six hours
277 before the 3rd-instar larvae to the end of the wandering larvae (the start of prepupa
278 stage). Stage 3 was from the start of prepupa stage to the end of the 2nd day of the
279 pupal stage. Stage 4 was from the end of the 2nd day of the pupal stage to the eclosion
280 of adults. The copulation rate did not change significantly when activating PTTH
281 neurons during the stage 1, stage 3 or stage 4 (**Figure 3B, 3D and 3E**). However, we
282 found the significant lower copulation rate and the longer latency to copulation only
283 when PTTH neurons were activated during the stage 2 (**Figure 3C and Figure 3F**). The
284 defected copulation was not due to a lower locomotion activity of virgin females (**Figure**
285 **3G**). Taken together, our findings indicated that the activity of dsx^{+} PTTH neurons
286 negatively regulate virgin female receptivity during the stage from the start of the 3rd-
287 instar to the end of wandering stage.
288
289 **PTTH modulates virgin female receptivity through ecdysone.**
290
291 The 3rd-intar larval stage is the critical stage for the initiation of metamorphosis involving
292 the synthesis of ecdysone (Imura et al., 2020; Lavrynenko et al., 2015; Shimell et al.,
293 2018). To test whether PTTH regulates virgin female receptivity through regulating the

294 synthesis of ecdysone, we rescued the enhanced female receptivity by feeding 20E to
295 the 3rd-intar larval *Ptth*^{Delete} flies. The enhanced copulation rate and shorter latency to
296 copulation of the *Ptth*^{Delete} flies were rescued to the comparable level of wild type
297 females (**Figure 4**). Furthermore, the wild type females fed by 20E had no significantly
298 different copulation rate and latency to copulation compared with the wild type females
299 fed by the same volume of 95% ethanol which is the solvent of 20E (**Figure 4**). This
300 suggested that PTTH regulates virgin female receptivity through the titer of ecdysone.
301
302 **Ecdysone receptor EcR-A in pC1 neurons regulates virgin female copulation rate.**
303
304 Given that PTTH regulates virgin female receptivity through ecdysone which acts on its
305 receptor EcR, we then asked whether ecdysone regulates the function of neurons
306 associated with virgin female receptivity through EcR. pC1 and vpoDN neurons are two
307 main dsx^{+} neurons involved in virgin female receptivity (Wang et al., 2021; Zhou et al.,
308 2014). pC1 neurons encode the mating status of female flies, vpoDN neurons regulate
309 the opening of vaginal plate when females attend to accept males. EcR-A and EcR-B1
310 are the two prominently expressed ecdysone receptors in the CNS (Riddiford et al.,
311 2000). First, we tested the expression of EcR-A and EcR-B1 in these two neurons on
312 the 2nd day of the pupal stage when ecdysone functions as the main mover in the
313 metamorphosis (Dalton et al., 2009; Truman et al., 1994). The GFP signals labeled by
314 pC1-ss2-Gal4 and vpoDN-ss1-Gal4 were merged well with the signals of both EcR-A
315 and EcR-B1 antibodies respectively (**Figure 5—figure supplement 1**). This revealed
316 that EcR-A and EcR-B1 express in both pC1 and vpoDN neurons. We then tested the

317 function of EcR in pC1 and vpoDN neurons through reducing the expression of EcR-A
318 and EcR-B1 respectively. We used the split-Gal4 for pC1 and vpoDN neurons to drive
319 the UAS-EcR-RNAi. First, we reduced the expression of all EcR isoforms in pC1
320 neurons, this decreased the copulation rate and prolonged the latency to copulation
321 significantly (**Figure 5—figure supplement 2A**). Furthermore, we reduced the
322 expression of EcR-A in pC1 neurons. The virgin female had the significant lower
323 copulation rate and longer latency to copulation (**Figure 5A**). The reduced copulation
324 rate had no relationship with the attractivity (**Figure 5E**) and the locomotion activity of
325 virgin females (**Figure 5—figure supplement 2B**). When reducing the expression of
326 EcR-B1 in pC1 neurons, virgin females had the significant longer latency to copulation
327 but the comparable copulation rate to controls (**Figure 5B**). However, reducing the
328 expression of EcR-A (**Figure 5—figure supplement 3A-C**) and EcR-B1 (**Figure 5—**
329 **figure supplement 3D-F**) using three split vpoDN-Gal4s in vpoDN neurons all did not
330 affect virgin female receptivity. This suggested that the expression of EcR-A in pC1
331 neurons regulates virgin female copulation rate, but EcR isoforms in vpoDN neurons do
332 not modulate virgin female receptivity.
333
334 Two split-Gal4 drivers for pC1 neurons had been obtained previously. pC1-ss1-Gal4
335 labels pC1-a, c and -e neurons, and pC1-ss2-Gal4 labels all pC1-a, -b, -c, -d and -e
336 neurons (Wang et al., 2020b). We also tested virgin female receptivity when EcR-A or
337 EcR-B1 were reduced in pC1-a, -c and -e neurons simultaneously using pC1-ss1-Gal4
338 respectively. While the copulation rate or the latency to copulation did not change
339 significantly (**Figure 5C-D**). This suggested that, pC1b only, or both pC1b and pC1d

340 neurons is necessary for the functions of EcR-A and EcR-B1 in pC1 neurons on virgin
341 female receptivity. Whether pC1d is involved in the regulation of female receptivity is
342 uncertain (Deutsch et al., 2020; Schretter et al., 2020; Taisz et al., 2023). However,
343 when reducing EcR-A in pC1d neurons alone using the specific split-Gal4 SS56987
344 (Schretter et al., 2020), virgin female receptivity including copulation rate and latency to
345 copulation did not change significantly compared with controls (**Figure 5—figure**
346 **supplement 4**). These results suggested that the function of EcR-A in pC1b neurons is
347 necessary for virgin female copulation rate.
348
349 As recently mated females may reduce sexual receptivity and increase egg laying (Avila
350 et al., 2011; Kubli, 2003). we asked whether the decreased copulation rate induced by
351 EcR-A could be a post-mating response and correlate with elevated egg laying. To
352 address this, we examined the number of eggs laid by virgin females when EcR-A was
353 reduced in pC1 neurons. We found that manipulation of EcR-A did not enhance egg
354 laying significantly in virgin females (**Figure 5F**), although the UAS-EcR-A-RNAi control
355 causes a massive decrease in female fertility. Meanwhile, we further analyzed whether
356 reduction of EcR-A in pC1 neurons regulates the opening of vaginal plate (VPO) or the
357 ovipositor extrusion (OE). We found that reducing the EcR-A expression in pC1 neurons
358 lead to the significantly less VPO and more OE (**Figure 5G-H**). These results suggested
359 that reduced EcR-A expression in pC1 neurons results in the similar phenotype to that
360 of mated females.
361
362 **EcR-A participates in the morphological development of pC1 neurons.**

363

364 EcR isoforms have distinct temporal and spatial expression patterns in the CNS
365 (Riddiford et al., 2000; Truman et al., 1994). It is unknown when EcR-A functions in pC1
366 neurons for virgin female receptivity. Thus, we examined virgin female receptivity when
367 EcR-A expression was conditionally reduced through RNAi via the pC1-ss2-Gal4 under
368 the control of the temporal and regional gene expression targeting system (McGuire et
369 al., 2004). EcR-A was reduced during the whole larval, pupal and adult stage
370 respectively (**Figure 5I-K**). When the experiment was done at the pupal stage is the
371 only situation when the controls were both different from the experimental (**Figure 5J**).
372 The result suggested that EcR-A in pC1 neurons plays a role in virgin female receptivity
373 during metamorphosis. This is consistent with that PTTH regulates virgin female
374 receptivity before the start of metamorphosis.

375

376 We then tested how EcR-A functions in pC1 neurons to modulate virgin female
377 receptivity. First, we tested the morphology of pC1 neurons when reducing the
378 expression of EcR-A in pC1 neurons. We found that the morphology of pC1-ss2-Gal4
379 expressing neurons appeared after the formation of the white pupa (Figure **6A1**). The
380 reduced EcR-A expression induced the more elaborated morphologies of the pC1-d/e
381 cells, especially the extra vertical projection (EVP) near the midline of brains (**Figure 6**
382 **B-D**) (Deutsch et al., 2020). These changes exhibited from the second day of the pupal
383 stage (**Figure 6B1-B2 and 6E**) and maintained at the adult stage (**Figure 6 D1-D2 and**
384 **6F**). Meanwhile, the number of pC1 cell bodies in adult flies when EcR-A was reduced
385 were the same as that of wild type flies (**Figure 6G**). Previous studies suggested that

386 pC1d cells serve as a hub within the central brain for dsx$^+$ and fru$^+$ neurons (Deutsch et
387 al., 2020). Thus, the abnormal development of pC1d neurons may induce the changes
388 between pC1d neurons and other dsx$^+$ and fru$^+$ neurons to affect associated behaviors.
389
390 Furthermore, we asked whether reduced female copulation rate was due to that EcR-A
391 expression affected the activity of pC1 neurons. Because all pC1 cells characterized so
392 far project to the lateral junction of the lateral protocerebral complex (LPC) (Kimura et
393 al., 2015; Rezával et al., 2016; Scheffer et al., 2020; Wang et al., 2020b; Wu et al.,
394 2019; Zhou et al., 2014), we expressed GCamp6s in all pC1 neurons and tested the
395 calcium signals in the lateral junction of LPC when EcR-A was knocked down (**Figure 6**
396 **D1-D2**). Reduced EcR-A did not induce significantly different calcium responses in the
397 LPC (**Figure 6H**). Thus, our results suggested that the decreased female copulation
398 rate induced by reduced EcR-A in pC1 neurons was mainly due to the morphological
399 changes of pC1b neurons, which then modulate the connections of pC1b neurons with
400 other neurons.
401
402 **The function of PTTH on EcR-A and pC1 neurons.**
403
404 As newly formed prepupae, the ptth-Gal4 > UAS-Grim flies display similar changes in
405 gene expression to the genetic control flies to response to a high-titer ecdysone pulse.
406 These genes include the repression of EcR (McBrayer et al., 2007). According to the
407 contradictory functions of PTTH deletion and EcR-A reduction in pC1 neurons, we
408 wanted to know whether there is a similar feedforward relationship between PTTH and

409 EcR-A. We quantified the EcR-A expression in the whole pupa body during the start of
410 prepupa stage, when the pC1-ss2-Gal4 expressing neurons appear. Indeed, PTTH -/-
411 induced upregulated EcR-A compared with PTTH -/+ flies (**Figure 7A**). This suggested
412 the feedforward relationship between PTTH and EcR-A expression during the start of
413 prepupa stage. Consistent with this, when PTTH was deleted, pC1 neurons exhibited
414 the contradictory pattern to that when EcR-A was decreased in pC1 neurons (**Figure**
415 **7B-C)**. These suggested the feedforward relationship between PTTH and EcR-A, and
416 may explain the contradictory functions of PTTH deletion and EcR-A reduction in pC1
417 neurons for female receptivity.
418
419 Furthermore, PTTH neurons are *dsx*-positive, almost all neurons regulating female
420 receptivity express Dsx^F. We wanted to know whether PTTH neurons affect other dsx^+
421 neurons, including pC1 neurons. Indeed, we detected the slightly overlap of dsx-
422 LexA>LexAop-RFP and torso-Gal4>UAS-GFP during larval stage (**Figure 7D**).
423 Furthermore, decreasing torso expression in pC1 neurons significantly inhibit female
424 receptivity (**Figure 7E**). The inhibited virgin female receptivity had no relationship either
425 with the locomotion activity of virgin females (**Figure 7F**). These results suggest that,
426 PTTH regulates female receptivity not only through ecdysone, but also may through
427 regulating other neurons especially Dsx^F-positive neurons associated with female
428 receptivity directly.
429
430 **Discussion**
431

432 In this study, we found that peptide hormone PTTH negatively modulates virgin female
433 receptivity through ecdysone. PTTH neurons are doublesex-positive and regulate virgin
434 female receptivity during neural development. PTTH deletion resulted in the increased
435 ecdysone receptor EcR-A expression in newly formed prepupae. Furthermore, EcR-A
436 functions in pC1 neurons to positively regulate virgin female receptivity during
437 metamorphosis mainly through modulating the anatomical morphology of pC1b
438 neurons. Additionally, decreasing the expression of PTTH receptor torso in pC1
439 neurons inhibited female receptivity. Taken together, our results revealed the contrary
440 functions of PTTH deletion and reduction of EcR-A in pC1 neurons during
441 neurodevelopment. In addition, EcR-A in pC1 neurons regulates virgin female
442 copulation rate during metamorphosis mainly through modulating the morphology of
443 pC1b neurons.
444
445 Most of neurons regulating sexual behaviors in female flies are dsx-positive. Our results
446 showed that PTTH neurons are also dsx^+ neurons. This suggested that PTTH neurons
447 have relationships with other dsx^+ neurons and the juvenile–adult transition is regulated
448 by *doublesex* gene. Indeed, we detected the overlap between torso-Gal4 signal and
449 dsx-LexA signal at the larval stage. Furthermore, when PTTH receptor torso was
450 decreased in dsx^+ pC1 neurons, female receptivity was inhibited. This suggested that
451 PTTH functions in pC1 neurons through neuronal projection or endocrine pathway
452 directly to regulate female receptivity. However, we did not detect the change of female
453 receptivity when Dsx^F was decreased in PTTH neurons. This suggested that Dsx^F

454 functions in PTTH neurons on other aspects, such as the development of PTTH
455 neurons or the synthesis and release of PTTH to regulate development.
456
457 PTTH regulates virgin female receptivity in an ecdysone-dependent manner before
458 metamorphosis. Ecdysone functions through its receptor EcR which is involved in all
459 phases of the nervous system development. In our study, reduced EcR-A expression in
460 all pC1 neurons, which encode the mating status of females, lead to the decreased
461 copulation rate. While, reduced EcR-A in pC1-a, c and e simultaneously did not reduce
462 the copulation rate significantly. This suggested that EcR-A plays the critical role in pC1-
463 b or/and -d neurons for regulating virgin female receptivity. Our results revealed that
464 reduced EcR-A induced the more elaborated morphologies of pC1d neurons. Previous
465 studies detected the synaptic connections between the axons of pC1d and the dendrites
466 of DNp13 neurons (Deutsch et al., 2020; Mezzera et al., 2020). DNp13 neurons are
467 command neurons for ovipositor extrusion. When females extruded, the ovipositor
468 physically impedes copulation (Mezzera et al., 2020; Wang et al., 2020a). However,
469 reduced EcR-A expression in pC1d neurons did not affect virgin female receptivity
470 (**Figure 5—figure supplement 4**). This might be due to three possibilities. First, the
471 more elaborated morphologies of pC1d neurons did not affect synaptic connections
472 between pC1d and DNp13 neurons. Second, the unchanged pC1 neural activity could
473 not affect the neural activity of DNp13 neurons. Third, the morphological change of
474 pC1d neurons is not sufficient for the decreased copulation rate. To sum, these suggest
475 that the morphological change of pC1b neurons is necessary for the decreased

476 copulation rate. However, due to the lack of pC1b drivers, we could not rule out
477 morphological changes in pC1b neurons when EcR-A was reduced.
478
479 In our study, PTTH negatively regulates female receptivity, while EcR-A positively
480 regulates female receptivity. Previous study revealed that, expression of EcR is
481 repressed in newly formed prepupae to response to high-titer ecdysone pulse
482 (Mcbrayer et al., 2007). We detected the similar feedforward relationship between PTTH
483 and EcR-A in newly formed prepupae. Consistent with this, we detected the contrary
484 pattern of pC1d neurons when PTTH was deleted, compare with that when EcR-A was
485 decreased in pC1 neurons. However, it is not sure that PTTH deletion could result in the
486 increased expression of EcR-A in pC1 neurons. In addition, PTTH deletion must affect
487 the development of almost other neurons, but not only pC1 neurons. This maybe the
488 reason for that reduction of Torso in pC1 neurons had contrary effect on female
489 receptivity to that when PTTH is deleted. So, the feedforward relationship between
490 PTTH and EcR-A in newly formed prepupae is one possible reason for the contrary
491 functions of PTTH deletion and reduction of EcR-A in pC1 neurons on female
492 receptivity.
493
494 Previous studies have demonstrated that the development of fru^+ neurons need EcR-A
495 in male *Drosophila melanogaster*. Furthermore, reduced EcR-A in fru^+ neurons induced
496 the male-male courtship (Dalton et al., 2009). We also detected the male-male courtship
497 behavior when PTTH was deleted (data not shown) as previous study (Mcbrayer et al.,
498 2007). This remits to the impact of ecdysone on dsx^+ or fru^+ neurons. Similarly, PTTH

deletion may also affect the development of other neurons and further other behaviors such as the female fecundity and the body size (Mcbrayer et al., 2007; Rewitz K F 2009; Shimell et al., 2018), although there is no sufficient evidence for the effects of fecundity and the body size on female receptivity. So, we could not exclude all effects of other aspects on female receptivity.

Our results suggested a regulatory role of PTTH in virgin female receptivity. Even though insects and mammals represent highly diverged classes, insects have evolved a similar strategy for triggering the juvenile–adult transition (Herbison, 2016; Pan et al., 2019). The juvenile–adult transition involves the hypothalamic–pituitary–gonadal (HPG) axis in mammals and the PG axis in insects. Among the neurons belonging to the axis, PTTH neurons and GnRH neurons have the similar function to stimulate the PG gland and pituitary gland to release hormones which trigger maturation, respectively. It will be interesting to study the function of GnRH neurons on the mammal sexual behaviors. This work extends the understanding of how neurodevelopmental processes regulate adult sexual behavior.

522 **Materials and methods**

Key Resources Table				
Reagent type (species) or resource	**Designation**	**Source or reference**	**Identifiers**	**Additional information**
antibody	Mouse anti-Bruchpilot antibody (nc82)	Developmental Studies Hybridoma Bank	Cat# nc82, RRID: AB_2314866	IHC (1:40)
antibody	Mouse Anti-Drosophila ecdysone receptor (EcR-A) Monoclonal Antibody	Developmental Studies Hybridoma Bank	Cat# 15G1a (EcR-A), RRID: AB_528214	IHC (1:10)
antibody	mouse Anti-Drosophila ecdysone receptor (EcR-B1) Antibody	Developmental Studies Hybridoma Bank	Cat# AD4.4(EcR-B1), RRID: AB_2154902	IHC (1:10)
antibody	Rabbit polyclonal anti-GFP	Thermo Fisher Scientific	Cat# A-11122, RRID: AB_221569	IHC (1:1000)
antibody	chicken polyclonal anti-GFP	Thermo Fisher Scientific	Cat# A10262, RRID: AB_2534023	IHC (1:1000)
antibody	Goat anti-rabbit, Alexa Fluor 488	Thermo Fisher Scientific	Cat# A-11034, RRID: AB_2576217	IHC (1:500)
antibody	Goat anti-chickent, Alexa Fluor 488	Thermo Fisher Scientific	Cat#A-11039; RRID: AB_2534096	IHC (1:500)
antibody	Goat anti-mouse, Alexa Fluor 488	Thermo Fisher Scientific	Cat# A-11029, RRID: AB_2534088	IHC (1:500)
antibody	Goat anti-rabbit, Alexa Fluor 546	Thermo Fisher Scientific	Cat# A-11010, RRID: AB_2534077	IHC (1:500)
antibody	Rabbit polyclonal anti-RFP	Thermo Fisher Scientific	Cat# R10367, RRID: AB_10563941	IHC (1:500)
antibody	Goat anti-mouse, Alexa Fluor 647	Thermo Fisher Scientific	Cat# A-21235, RRID: AB_2535804	IHC (1:500)
antibody	Rabbit polyclonal anti-PTTH	Zhou Lab, Chinese Academy of Sciences, this paper	N/A	IHC (1:1300)
chemical compound, drug	Paraformaldehyde (PFA)	Electron Microscopy Sciences	Cat#15713	8% PFA diluted in 1XPBS at 1:4 or 1:2
chemical compound, drug	DPX Mountant	Sigma-Aldrich	Cat#44581	
chemical compound, drug	Normal goat serum	Sigma-Aldrich	Cat#G9023	
chemical compound, drug	20-hydroxyecdysone	Cayman	Cat#16145	dissolved in 95% ethanol, 0.2 mg/ml
chemical compound, drug	TRIzol	Ambion	Cat#15596018	
Genetic reagent (*D.melanogaster)*	*LexAop2-mCD8::GFP*	Bloomington Stock Center	BL#32203	
Genetic reagent (*D.melanogaster)*	*;;UAS-mCD8::GFP*	Bloomington Stock Center	BL#32194	
Genetic reagent (*D.melanogaster)*	*;UAS-mCD8::GFP;*	Bloomington Stock Center	BL#5137	
Genetic reagent (*D.melanogaster)*	*UAS-dTrpA1/cyo*	Garrity Lab, Brandeis University	N/A	

Genetic reagent (*D.melanogaster)*	*UAS-Kir2.1*	Bloomington Stock Center	BL#6595	
Genetic reagent (*D.melanogaster)*	*Ptth-Gal4*	Rao Lab, Peking University	N/A	
Genetic reagent (*D.melanogaster)*	*PtthLexA*	Rao Lab, Peking University	N/A	
Genetic reagent (*D.melanogaster)*	*⊿PTTH*	Rao Lab, Peking University	N/A	
Genetic reagent (*D.melanogaster)*	*UAS-PTTH*	Zhou Lab, Chinese Academy of Sciences, this paper	N/A	
Genetic reagent (*D.melanogaster)*	*isoCS*	Rao Lab, Peking University	N/A	
Genetic reagent (*D.melanogaster)*	*elav-Gal4*	Rao Lab, Peking University	N/A	
Genetic reagent (*D.melanogaster)*	*UAS-GFPStinger*	Janelia Research Campus	N/A	
Genetic reagent (*D.melanogaster)*	*LexAop-tomato*	Janelia Research Campus	N/A	
Genetic reagent (*D.melanogaster)*	*LexAop2-FlpL*	Janelia Research Campus	N/A	
Genetic reagent (*D.melanogaster)*	*UAS > stop > mCD8-GFP*	Janelia Research Campus	N/A	
Genetic reagent (*D.melanogaster)*	*Dsx-Gal4*	Janelia Research Campus	N/A	
Genetic reagent (*D.melanogaster)*	*Dsx-LexA*	Janelia Research Campus	N/A	
Genetic reagent (*D.melanogaster)*	*tub-Gal80^{ts}*	Pan Lab, Southeast University	BL#7018	
Genetic reagent (*D.melanogaster)*	*pC1-ss1-Gal4*	Wang Lab, Lingang Laboratory	N/A	
Genetic reagent (*D.melanogaster)*	*pC1-ss2- Gal4*	Wang Lab, Lingang Laboratory	N/A	
Genetic reagent (*D.melanogaster)*	*vpoDN-ss1-Gal4*	Wang Lab, Lingang Laboratory	N/A	
Genetic reagent (*D.melanogaster)*	*vpoDN-ss2-Gal4*	Wang Lab, Lingang Laboratory	N/A	
Genetic reagent (*D.melanogaster)*	*vpoDN-ss3-Gal4*	Wang Lab, Lingang Laboratory	N/A	
Genetic reagent (*D.melanogaster)*	*UAS-EcR-RNAi*	Bloomington Stock Center	BL#9327	
Genetic reagent (*D.melanogaster)*	*UAS-EcR-A-RNAi*	Bloomington Stock Center	BL#9328	
Genetic reagent (*D.melanogaster)*	*UAS-EcR-B1-RNAi*	Bloomington Stock Center	BL#9329	
Genetic reagent (*D.melanogaster)*	*pC1d-Gal4*	Bloomington Stock Center	BL#86847	

Genetic reagent (*D.melanogaster)*	*UAS-PTTH-RNAi*	VDRC	V102043	
Genetic reagent (*D.melanogaster)*	*UAS-Dsx^F-RNAi*	Pan Lab	N/A	
Genetic reagent (*D.melanogaster)*	*UAS-Torso-RNAi*	Liu Lab	BL#33627	
recombinant DNA reagent	pBSK-attP-3P3-RFP-loxP	Bowen Deng et al., 2019	N/A	
recombinant DNA reagent	pBSK-attB-loxP-myc-T2A-Gal4Gal4-GMR-miniwhite	Bowen Deng et al., 2019	N/A	
recombinant DNA reagent	pBSK-attB-loxP-V5-T2A-LexA::p65-GMR-miniwhite	Bowen Deng et al., 2019	N/A	
software, algorithm	MATLAB	MathWorks, Natick, MA	https://www.mathworks.com/products/matlab.html	
software, algorithm	ImageJ	National Institutes of Health	https://imagej.nih.gov/ij/	
software, algorithm	Prism 7	GraphPad	https://www.graphpad.com/	
software, algorithm	R 4.1.3	RStudio	https://www.r-project.org	

Fly stocks

Flies were reared on standard cornmeal-yeast medium under a 12 hr:12 hr dark:light cycle at 25°C and 60% humidity. All the knock-out lines in this study for screening have been published [49]. The following strains were obtained from Dr. Yi Rao: *isoCS* (wild-type), *ΔPtth*, *Ptth-Gal4, Ptth-LexA, elav-Gal4 and UAS-Kir2.1* (BL#6595). UAS-dTrpA1 was a gift from Dr. Paul Garrity. *UAS-GFPStinger*, *LexAop-tomato, LexAop2-FlpL, UAS > stop > mCD8-GFP*, *dsx-Gal4* and *dsx-LexA* (Mellert et al., 2010) have been described previously (Pfeiffer et al., 2008; Pfeiffer et al., 2010) and are obtained from Janelia Research Campus. *tub-Gal80^{ts}* (BL#7018) was provided by Dr. Yufeng Pan. *pC1-ss1-Gal4, pC1-ss2-Gal4, vpoDN-ss1-Gal4, vpoDN-ss2-Gal4* and *vpoDN-ss3-Gal4* were provided by Dr. Kaiyu Wang. *Torso-RNAi* (BL#33627) was a gift from Suning Liu. The following lines were obtained from the Bloomington Drosophila Stock Center: *UAS-EcR-RNAi* (BL#9327), *UAS-EcR-A-RNAi* (BL#9328), *UAS-EcR-B1-RNAi* (BL#9329),

538 *UAS-mCD8::GFP* (BL#32194), *LexAop2-mCD8::GFP* (BL#32203), *UAS-mCD8::GFP*
539 (BL#5137) and *pC1d-Gal4* (BL#86847). *UAS-PTTH-RNAi* (v102043) was from Vienna
540 Drosophila Resource Center (VDRC).
541
542 **Behavioral assays**
543
544 Flies were reared at 25°C and 60% humidity under a 12 hr light:12 hr dark cycle. Virgin
545 females and wild-type males were collected upon eclosion, placed in groups of 12 flies
546 each and aged 4–6 days (except for the assays for PTTH mutant on different days after
547 eclosion, and the molecular rescue assay for the 24h-old females) before carrying out
548 behavioral assay except for the transient thermogenetic experiments. Female receptivity
549 assays were conducted as previously described (Wang et al., 2022; Zhou et al., 2014).
550 A virgin female of defined genotype and a wild type male were gently cold anesthetized
551 and respectively introduced into two layers of the courtship chambers separated by a
552 removable transparent film. The flies were allowed to recover for at least 45 min before
553 the film was removed to allow the pair of flies to contact. The mating behavior was
554 recorded using a camera (Canon VIXIA HF R500) for 30 min at 17 fps for further
555 analysis.
556
557 For transient activation experiment by dTrpA1 in adult stage, flies were reared at 23°C.
558 Flies were loaded into courtship chamber and recovered for at least 30 min at 23°C,
559 then were placed at 23°C (control group) or 29°C (experimental group) for 30 min prior
560 to removing the film and videotaping. For activation experiment by dTrpA1 during

561 development, flies were reared at 29°C during the specific stages compared with the
562 controls who were reared at 23°C all the time. Flies were loaded into courtship chamber
563 and recovered for at least 45 min at 23°C prior to removing the film and videotaping.
564
565 **Quantification and statistical analysis of female receptivity behavior**
566
567 Two parameters including copulation rate and latency to copulation were used to
568 characterize receptivity and we got the data sets of two parameters from the same flies.
569 The time from removing the film to successful copulation was measured for each
570 female. The number of females that had engaged in copulation by the end of each 1
571 min interval within 30 min were summed and plotted as a percentage of successful
572 copulation. The latency to copulation was the time from removing the film to successful
573 copulation. All the time points that female successfully copulated were manually
574 analyzed and the data of unhealthy flies were discarded.
575
576 **Temporally restricted RNAi**
577
578 tub-Gal80^{ts} crosses were reared at either 18°C for control groups or 30°C for
579 experimental groups. Virgin females were collected at eclosion and were placed in
580 groups of 12 flies each and aged 4–6 days before carrying out behavior assay. Assays
581 were tested at 23°C.
582
583 **Male courtship index**

584

585 Courtship index was defined as the proportion of time the male followed, oriented
586 toward and attempted to copulate the female within 5 min of courtship initiation, marked
587 by the initial orientation toward and following the female.

588

589 **Vaginal plate opening and ovipositor extrusion**

590

591 A virgin female of defined genotype and a wild type male were aspirated into the
592 courtship chambers and respectively introduced into two layers of the courtship
593 chambers separated by a removable transparent film. The flies were allowed to recover
594 for 30 min before the film was removed. To allow visualization of vaginal plate opening,
595 we recorded uncompressed image sequences at 896 x 896 pixels and 50 frames per
596 second using a Photron Mini AX camera (Photron) with an AF-S VR Micro-Nikkor
597 105mm lens (Nikon). Instances of vaginal plate opening and ovipositor extrusion were
598 scored blind to genotype from frame by-frame playback during the first 5 min of
599 courtship or until copulation if it occurred within 5 min. Courtship initiation was defined
600 as the male orienting toward and beginning to follow the female. Rare trials with fewer
601 than 30 s of total courtship were discarded.

602

603 **Locomotion assays**

604

605 The rearing and experimental conditions in locomotion assays were the same as that in
606 the corresponding female receptivity assays, excepting that individual females were

607 loaded in the chambers without males. Spontaneous movements of the flies were
608 recorded with a camera (Canon VIXIA HF R500) for 30 min at 30 fps for further
609 analysis. The activity of flies during the middle 10 min was analyzed to calculate the
610 average walking speed using Ctrax software.
611
612 **Egg Laying**
613
614 Virgin females were collected upon eclosion and one fly was housed on standard
615 medium at 25°C, 60% relative humidity, 12 hr light:12 hr dark and allowed to lay eggs in
616 single vials. Each fly was transferred into new food tube every 24 hr. The number of
617 eggs was counted at the end of each 24 hr period. The numbers during the 3rd and 4th
618 day were summed for statistics and plot.
619
620 **Immunohistochemistry**
621
622 Whole brains of flies were dissected in 1x PBS and fixed in 2% paraformaldehyde
623 diluted in 1x PBS for 55 min at room temperature. The samples were washed with PBT
624 (1x PBS containing 0.3% Triton X-100) for 1 hour (3 x 20 min), followed by blocking in
625 5% normal goat serum (Blocking solution, diluted in 0.3% PBT) for 1 hour at room
626 temperature. Then, the samples were incubated in primary antibodies (diluted in
627 blocking solution) for 18–24 hours at 4°C. Samples were washed with 0.3% PBT for 1
628 hour (3 x 20 min), then were incubated in secondary antibodies (diluted in blocking
629 solution) for 18–24 hours at 4°C. Samples were washed with 0.3% PBT for 1 hour (3 x

630 20 min), then were fixed in 4% paraformaldehyde for 4 hours at room temperature. After
631 washed with 0.3% PBT for 1 hour (3 x 20 min), brains were mounted on poly-L-lysine-
632 coated coverslip in 1x PBS. The coverslip was dipped for 5 min with ethanol of
633 30%→50%→70%→95%→100% sequentially at room temperature, and then dipped for
634 5 min three times with xylene. Finally, brains were mounted with DPX and allowed DPX
635 to dry for 2 days before imaging. Primary antibodies used were: chicken anti-GFP
636 (1:1000; Life Technologies #A10262), rabbit anti-GFP (1:1000; Life Technologies
637 #A11122), rabbit anti-RFP (1:1000; Life Technologies #R10367), rabbit anti-PTTH
638 antibody (1:1300), mouse anti-nc82 (1:40; DSHB), mouse anti-EcR-A (1:10;
639 AB_528214) and mouse anti-EcR-B1 (1:10; AB_2154902). Secondary antibodies used
640 were: Alexa Fluor goat anti-chicken 488 (1:500; Life Technologies #A11039), Alexa
641 Fluor goat anti-rabbit 488 (1:500; Life Technologies #A11034), Alexa Fluor goat anti-
642 rabbit 546 (1:500; Life Technologies #A11010), Alexa Fluor goat anti-mouse 647 (1:500;
643 Life Technologies #A21235), and Alexa Fluor goat anti-mouse 488 (1:500; Life
644 Technologies #A11029).
645
646 **Confocal microscopy and image analysis**
647
648 Confocal imaging was performed under an LSM 710 inverted confocal microscope
649 (ZEISS, Germany), with a Plan-Apochromat 20×/0.8 M27 objective or an EC Plan-
650 Neofluar 40x/1.30 oil DIC M27 objective, and later analyzed using Fiji software.
651
652 **Generation of anti-PTTH antibody**

653

654 The antisera used to recognize PTTH peptide were raised in New Zealand white rabbits
655 using the synthetic peptide N'- TSQSDHPYSWMNKDQPWQFKC -C'. The synthesis of
656 antigen peptide, the production and purification of antiserum were performed by Beijing
657 Genomics Institute (BGI).

658

659 **Generation of UAS-PTTH**

660

661 pJFRC28-5XUAS-IVS-GFP-p10 (#12073; Fungene Biotechnology, Shanghai, China)
662 was used for the generation of the pJFRC28-UAS-PTTH construct. The pJFRC28-
663 10XUAS-IVS-GFP-p10 plasmid was digested with NotI and XbaI to remove the GFP
664 coding sequence, and then the cDNA of PTTH was cloned into this plasmid by Gibson
665 Assembly. The Kozak sequence was added right upstream of the ATG. UAS-PTTH
666 constructs were injected and integrated into the attP2 site on the third chromosome
667 through phiC31 integrase mediated transgenesis. The construct was confirmed using
668 DNA sequencing through PCR. The primers used for cloning PTTH cDNA were as
669 follows:
670 UAS-PTTH-F
671 ATTCTTATCCTTTACTTCAGGCGGCCGCAAAATGGATATAAAAGTATGGCGACTCC
672 UAS-PTTH-R
673 GTTATTTTAAAAACGATTCATTCTAGATCACTTTGTGCAGAAGCAGCCG

674

675 **Genomic DNA extraction and RT-PCR**

676

677 Genomic DNA was extracted from 10 whole bodies of wandering flies using MightyPrep
678 reagent for DNA (Takara #9182). Whole body RNA was extracted from 10 whole bodies
679 of wandering flies using TRIzol (Ambion #15596018). cDNA was generated from total
680 RNA using the Prime Script reagent kit (Takara #RR047A). Candidates of *ΔPtth* were
681 characterized by the loss of DNA band in the deleted areas through PCR on the
682 genomic DNA and cDNA. Primer sequences used in Figure 1 are listed in **Table S1**.

683

684 **Measurements of pupariation timing and adult mass**

685

686 The flies were reared at 25°C and 60% humidity under a 12 hr light:12 hr dark cycle.
687 Two-hour time collections of embryos laid on standard food vials. Each vial contained
688 20-30 eggs. The range of time for pupariation were recorded for each vial. Sexed adults
689 of 24h-old were weighted in groups of ten flies using a NENVER-TP-214 microbalance
690 at the same time.

691

692 **Identification of sex in *Drosophila* larvae**

693

694 Third instar larvae can be sexed (True et al., 2014). Gonads are translucent and visible
695 in side view in the posterior third of the larva. The male gonads are about five times
696 bigger than the female gonads. The identified wandering female and male larvae were
697 reared in different vials for the subsequent experiments.

698

699 **Rescue by 20-hydroxyecdysone feeding**

700

701 Thirty freshly ecdysed *ΔPtth* L3 larvae, grown at 25°C and 60% humidity under a 12 hr
702 light:12 hr dark cycle, were washed with water and transferred to normal food for
703 additional aging. After 20 h, larvae were washed and transferred to a vial supplemented
704 with either 20-hydroxyecdysone (20E, Cayman #16145, dissolved in 95% ethanol, final
705 concentration 0.2 mg/ml) or 95% ethanol (same volume as 20E). The wild type larvae
706 were directly transferred to vials supplemented with 20E or 95% ethanol upon L3
707 ecdysis. Once seeded with L3 larvae, the vials were returned to 25°C and 60% humidity
708 under a 12 hr light:12 hr dark cycle.

709

710 **Quantification of fluorescence intensity**

711

712 The fluorescence intensity was quantified using Fiji software. The areas of interest
713 (ROI) were marked in the slices including the interested regions and quantified using
714 the “plot z-axis profile” function. The fluorescence intensity in each slice was summed
715 for statistics and plot. The parameters used for confocal imaging of each brain were the
716 same.

717

718 **Calcium imaging**

719

720 Flies aged 4-6-days were immobilized on ice for ~30 s. The brain was then dissected
721 out in extra-cellular solution (ECS) that contains (in millimoles): 108 NaCl, 5 KC1, 5

722 trehalose, 5 sucrose, 5 HEPES, 26 $NaHCO_3$, 1 NaH_2PO_4, 2 $CaCl_2$, and 1.5 $MgCl_2$ [pH
723 7.1 – 7.3 when bubbled with 95% (vol/vol) O_2/5% (vol/vol) CO_2, ~290 mOsm] and
724 mounted on a poly-D-lysine coated coverslip. The samples were continuously perfused
725 with ECS.
726
727 Calcium imaging was performed at 21°C on a customized two-photon microscope
728 equipped with a resonant scanner (Nikon), a piezo objective scanner (Nikon) and a 40x
729 water-immersion objective (Nikon). GCaMP6s was excited at 920 nm.
730
731 Analysis of calcium imaging data was done offline with NIS-Elements AR 5.30.01.
732 Briefly, the square region of interest (ROIs), 25 pixels on the pC1 neurons in the center
733 of lateral junction, was chosen for measurements. For each frame, the average
734 fluorescence intensity of pixels within ROIs was calculated blind to genotype. The
735 average fluorescence intensity of ROIs in each frame covering pC1 neurons were
736 summed for statistics and plot.
737
738 **qRT-PCR**
739
740 Total RNA was extracted from about 10 flies using TRIzol (Ambion #15596018). The
741 cDNA was synthesized using Prime Script reagent kit (Takara #RR047A). Quantitative
742 PCR was performed on Thermo Piko Real 96 (Thermo) using SYBR Green PCR Master
743 Mix (Takara #RR820A). The mRNA expression level was calculated by the $2^{-\Delta\Delta Ct}$
744 method and the results were plotted by using tubulin as the reference gene. Primers are

745 listed in **Table S1**. All reactions were performed in triplicate. The average of four
746 biological replicates ± SEM was plotted.
747
748 **Statistical analysis**
749
750 Statistical analyses were carried out using R software version 3.4.3 or Prism7
751 (GraphPad software). For the copulation rate, chi-square test is applied. The Mann-
752 Whitney U test was applied for analyzing the significance of two columns. Kruskal-
753 Wallis ANOVA test followed by post-hoc Mann-Whitney U test, was used to identify
754 significant differences between multiple groups.
755
756 **Data, Materials, and Software Availability**
757
758 All study data are included in the main text and supporting information, except for the
759 sequence data of RNAseq (**Supplementary File 3**) has been deposited in the Genome
760 Sequence Archive under the accession number CRA012130 in PRJCA018750. This
761 study does not involve new code. Fly stocks and reagents used in this study are
762 available from the corresponding author upon reasonable request.
763
764 **Acknowledgments**
765
766 We thank Yi Rao (Peking University), Yufeng Pan (Southeast University), Kaiyu Wang
767 (Lingang Laboratory), Yan Zhu (Chinese Academy of Sciences), Paul Garrity (Brandeis

University), Wei Zhang (Tsinghua University), Li Liu (Chinese Academy of Sciences), Suning Liu (South China Normal University) and Xuan Guo (Jinzhou Medical University), the Bloomington Drosophila Stock Center and Tsinghua Fly Center for sharing fly strains; Chenzhu Wang (Chinese Academy of Sciences), Yufeng Pan (Southeast University), Zhiqiang Yan (Shenzhen Bay Laboratory) and Yan Zhu (Chinese Academy of Sciences) for their comments; Xiangdong Li (Chinese Academy of Sciences), Fengming Wu (Chinese Academy of Sciences), Tao Wang (Chinese Academy of Sciences) and Jin Ge (Chinese Academy of Sciences) for assistance with behavioral assays; Yihui Chen and Hongjiang Gao for the maintenance of materials; other members of the Zhou laboratory for helpful discussions.

References

Avila F W, Sirot L K, LaFlamme B A, Rubinstein C D, & Wolfner M F. (2011). Insect seminal fluid proteins: identification and function. *Annu Rev Entomol, 56*, 21-40. doi:10.1146/annurev-ento-120709-144823

Billeter J C, Villella A, Allendorfer J B, Dornan A J, Richardson M, Gailey D A, & Goodwin S F. (2006). Isoform-specific control of male neuronal differentiation and behavior in Drosophila by the fruitless gene. *Curr Biol, 16*(11), 1063-1076. doi:10.1016/j.cub.2006.04.039

Clowney E J, Iguchi S, Bussell J J, Scheer E, & Ruta V. (2015). Multimodal chemosensory circuits controlling male courtship in Drosophila. *Neuron, 87*(5), 1036-1049. doi:10.1016/j.neuron.2015.07.025

Connolly K, & Cook R. (1973). Rejection responses by female drosophila-melanogaster - their ontogeny, causality and effects upon behavior of courting male. *Behaviour, 44*(1-2), 142-166. doi:10.1163/156853973x00364

Dai J D, & Gilbert L I. (1991). Metamorphosis of the corpus allatum and degeneration of the prothoracic glands during the larval-pupal-adult transformation of Drosophila melanogaster: a cytophysiological analysis of the ring gland. *Dev Biol, 144*(2), 309-326. doi:10.1016/0012-1606(91)90424-2

Dalton J E, Lebo M S, Sanders L E, Sun F, & Arbeitman M N. (2009). Ecdysone receptor acts in fruitless- expressing neurons to mediate drosophila courtship behaviors. *Curr Biol, 19*(17), 1447-1452. doi:10.1016/j.cub.2009.06.063

800 Demir E, & Dickson B J. (2005). fruitless splicing specifies male courtship behavior in Drosophila.
801 *Cell, 121*(5), 785-794. doi:10.1016/j.cell.2005.04.027
802 Deng B, Li Q, Liu X, Cao Y, Li B, Qian Y, Xu R, Mao R, Zhou E, Zhang W, Huang J, & Rao Y. (2019).
803 Chemoconnectomics: mapping chemical transmission in Drosophila. *Neuron, 101*(5),
804 876-893.e874. doi:10.1016/j.neuron.2019.01.045
805 Deutsch D, Pacheco D, Encarnacion-Rivera L, Pereira T, Fathy R, Clemens J, Girardin C, Calhoun
806 A, Ireland E, Burke A, Dorkenwald S, McKellar C, Macrina T, Lu R, Lee K, Kemnitz N, Ih D,
807 Castro M, Halageri A, Jordan C, Silversmith W, Wu J, Seung H S, & Murthy M. (2020). The
808 neural basis for a persistent internal state in Drosophila females. *Elife, 9*.
809 doi:10.7554/eLife.59502
810 Dickson B J. (2008). Wired for sex: the neurobiology of Drosophila mating decisions. *Science,*
811 *322*(5903), 904-909. doi:10.1126/science.1159276
812 Feng K, Palfreyman M T, Hasemeyer M, Talsma A, & Dickson B J. (2014). Ascending SAG neurons
813 control sexual receptivity of Drosophila females. *Neuron, 83*(1), 135-148.
814 doi:10.1016/j.neuron.2014.05.017
815 Ferveur J F. (2010). Drosophila female courtship and mating behaviors: sensory signals, genes,
816 neural structures and evolution. *Curr Opin Neurobiol, 20*(6), 764-769.
817 doi:10.1016/j.conb.2010.09.007
818 Fuyama Y, & Ueyama M. (1997). Ovulation and the suppression of mating in Drosophila
819 melanogaster females: behavioral basis. *Behav Genet, 27*(5), 483-488.
820 doi:10.1023/a:1025630602057
821 Ganter G K, Walton K L, Merriman J O, Salmon M V, Brooks K M, Maddula S, & Kravitz E A.
822 (2007). Increased male-male courtship in ecdysone receptor deficient adult flies. *Behav*
823 *Genet, 37*(3), 507-512. doi:10.1007/s10519-006-9140-1
824 Greenspan R J, & Ferveur J F. (2000). Courtship in Drosophila. *Annu Rev Genet, 34*, 205-232.
825 doi:10.1146/annurev.genet.34.1.205
826 Hall J. (1978). Courtship among males due to a male-sterile mutation inDrosophila
827 melanogaster. *Behavior Genetics*(8-2).
828 Hall J C. (1994). The mating of a fly. *Science, 264*(5166), 1702-1714.
829 doi:10.1126/science.8209251
830 Hamada F N, Rosenzweig M, Kang K, Pulver S R, Ghezzi A, Jegla T J, & Garrity P A. (2008). An
831 internal thermal sensor controlling temperature preference in Drosophila. *Nature,*
832 *454*(7201), 217-220. doi:10.1038/nature07001
833 Häsemeyer M, Yapici N, Heberlein U, & Dickson B J. (2009). Sensory neurons in the Drosophila
834 genital tract regulate female reproductive behavior. *Neuron, 61*(4), 511-518.
835 doi:10.1016/j.neuron.2009.01.009
836 Herbison A E. (2016). Control of puberty onset and fertility by gonadotropin-releasing hormone
837 neurons. *Nat Rev Endocrinol, 12*(8), 452-466. doi:10.1038/nrendo.2016.70
838 Hoopfer E D, Jung Y, Inagaki H K, Rubin G M, & Anderson D J. (2015). P1 interneurons promote a
839 persistent internal state that enhances inter-male aggression in Drosophila. *Elife, 4*.
840 doi:10.7554/eLife.11346
841 Imura E, Shimada-Niwa Y, Nishimura T, Huckesfeld S, Schlegel P, Ohhara Y, Kondo S, Tanimoto
842 H, Cardona A, Pankratz M J, & Niwa R. (2020). The Corazonin-PTTH Neuronal Axis
843 Controls Systemic Body Growth by Regulating Basal Ecdysteroid Biosynthesis in

Drosophila melanogaster. *Curr Biol, 30*(11), 2156-2165 e2155. doi:10.1016/j.cub.2020.03.050

Ishimoto H, & Kamikouchi A. (2020). A feedforward circuit regulates action selection of pre-mating courtship behavior in female Drosophila. *Curr Biol, 30*(3), 396-407.e394. doi:10.1016/j.cub.2019.11.065

Ito H, Sato K, Koganezawa M, Ote M, Matsumoto K, Hama C, & Yamamoto D. (2012). Fruitless recruits two antagonistic chromatin factors to establish single-neuron sexual dimorphism. *Cell, 149*(6), 1327-1338. doi:10.1016/j.cell.2012.04.025

Jang Y H, Chae H S, & Kim Y J. (2017). Female-specific myoinhibitory peptide neurons regulate mating receptivity in Drosophila melanogaster. *Nat Commun, 8*(1), 1630. doi:10.1038/s41467-017-01794-9

Kimura K, Hachiya T, Koganezawa M, Tazawa T, & Yamamoto D. (2008). Fruitless and doublesex coordinate to generate male-specific neurons that can initiate courtship. *Neuron, 59*(5), 759-769. doi:10.1016/j.neuron.2008.06.007

Kimura K, Sato C, Koganezawa M, & Yamamoto D. (2015). Drosophila ovipositor extension in mating behavior and egg deposition involves distinct sets of brain interneurons. *PLoS One, 10*(5), e0126445. doi:10.1371/journal.pone.0126445

Kohatsu S, Koganezawa M, & Yamamoto D. (2011). Female contact activates male-specific interneurons that trigger stereotypic courtship behavior in Drosophila. *Neuron, 69*(3), 498-508. doi:10.1016/j.neuron.2010.12.017

Kubli E. (2003). Sex-peptides: seminal peptides of the Drosophila male. *Cell Mol Life Sci, 60*(8), 1689-1704. doi:10.1007/s00018-003-3052

Kurtovic A, Widmer A, & Dickson B J. (2007). A single class of olfactory neurons mediates behavioural responses to a Drosophila sex pheromone. *Nature, 446*(7135), 542-546. doi:10.1038/nature05672

Kvitsiani D, & Dickson B J. (2006). Shared neural circuitry for female and male sexual behaviours in Drosophila. *Curr Biol, 16*(10), R355-356. doi:10.1016/j.cub.2006.04.025

Lavrynenko O, Rodenfels J, Carvalho M, Dye N A, Lafont R, Eaton S, & Shevchenko A. (2015). The ecdysteroidome of Drosophila: influence of diet and development. *Development, 142*(21), 3758-3768. doi:10.1242/dev.124982

Ma B, Wang R, Liu Y, Deng B, Wang T, Wu F, & Zhou C. (2022). Serotonin signaling modulates sexual receptivity of virgin female Drosophila. *Neurosci Bull, 38*(11), 1277-1291. doi:10.1007/s12264-022-00908-8

Manoli D S, Fan P, Fraser E J, & Shah N M. (2013). Neural control of sexually dimorphic behaviors. *Curr Opin Neurobiol, 23*(3), 330-338. doi:10.1016/j.conb.2013.04.005

Manoli D S, Foss M, Villella A, Taylor B J, Hall J C, & Baker B S. (2005). Male-specific fruitless specifies the neural substrates of Drosophila courtship behaviour. *Nature, 436*(7049), 395-400. doi:10.1038/nature03859

Manoli D S, Meissner G W, & Baker B S. (2006). Blueprints for behavior: genetic specification of neural circuitry for innate behaviors. *Trends Neurosci, 29*(8), 444-451. doi:10.1016/j.tins.2006.06.006

McBrayer Z, Ono H, Shimell M, Parvy J P, Beckstead R B, Warren J T, Thummel C S, Dauphin-Villemant C, Gilbert L I, & O'Connor M B. (2007). Prothoracicotropic hormone regulates

887 developmental timing and body size in Drosophila. *Dev Cell, 13*(6), 857-871.
888 doi:10.1016/j.devcel.2007.11.003
889 McGuire S E, Mao Z, & Davis R L. (2004). Spatiotemporal gene expression targeting with the
890 TARGET and gene-switch systems in Drosophila. *Sci STKE, 2004*(220), pl6.
891 doi:10.1126/stke.2202004pl6
892 Mellert D J, Knapp J M, Manoli D S, Meissner G W, & Baker B S. (2010). Midline crossing by
893 gustatory receptor neuron axons is regulated by fruitless, doublesex and the
894 Roundabout receptors. *Development, 137*(2), 323-332. doi:10.1242/dev.045047
895 Mellert D J, Robinett C C, & Baker B S. (2012). doublesex functions early and late in gustatory
896 sense organ development. *PLoS One, 7*(12), e51489. doi:10.1371/journal.pone.0051489
897 Mezzera C, Brotas M, Gaspar M, Pavlou H J, Goodwin S F, & Vasconcelos M L. (2020). Ovipositor
898 extrusion promotes the transition from courtship to copulation and signals female
899 acceptance in Drosophila melanogaster. *Curr Biol, 30*(19), 3736-3748.e3735.
900 doi:10.1016/j.cub.2020.06.071
901 Neckameyer W S. (1998). Dopamine modulates female sexual receptivity in Drosophila
902 melanogaster. *J Neurogenet, 12*(2), 101-114. doi:10.3109/01677069809167259
903 Naoki Yamanaka, Nuria M Romero, Francisco A Martin, Kim F Rewitz, Mu Sun, Michael B
904 O'Connor, Pierre Léopold. (2013). Neuroendocrine Control of Drosophila larval light
905 preference. *Science*, 41(6150), 1113-1116. doi: 10.1126/science.1241210
906 Pan X, & O'Connor M B. (2019). Developmental Maturation: Drosophila AstA signaling provides
907 a kiss to grow up. *Curr Biol, 29*(5), R161-R164. doi:10.1016/j.cub.2019.01.040
908 Pan Y, & Baker B S. (2014). Genetic identification and separation of innate and experience-
909 dependent courtship behaviors in Drosophila. *Cell, 156*(1-2), 236-248.
910 doi:10.1016/j.cell.2013.11.041
911 Pan Y, Meissner G W, & Baker B S. (2012). Joint control of Drosophila male courtship behavior
912 by motion cues and activation of male-specific P1 neurons. *PNAS, 109*(25), 10065-
913 10070. doi:10.1073/pnas.1207107109
914 Pan Y, Robinett C C, & Baker B S. (2011). Turning males on: activation of male courtship
915 behavior in Drosophila melanogaster. *PLoS One, 6*(6), e21144.
916 doi:10.1371/journal.pone.0021144
917 Pavlou H J, & Goodwin S F. (2013). Courtship behavior in Drosophila melanogaster: towards a
918 'courtship connectome'. *Curr Opin Neurobiol, 23*(1), 76-83.
919 doi:10.1016/j.conb.2012.09.002
920 Pfeiffer B D, Jenett A, Hammonds A S, Ngo T T, Misra S, Murphy C, Scully A, Carlson J W, Wan K
921 H, Laverty T R, Mungall C, Svirskas R, Kadonaga J T, Doe C Q, Eisen M B, Celniker S E, &
922 Rubin G M. (2008). Tools for neuroanatomy and neurogenetics in Drosophila. *PNAS,*
923 *105*(28), 9715-9720. doi:10.1073/pnas.0803697105
924 Pfeiffer B D, Ngo T T, Hibbard K L, Murphy C, Jenett A, Truman J W, & Rubin G M. (2010).
925 Refinement of tools for targeted gene expression in Drosophila. *Genetics, 186*(2), 735-
926 755. doi:10.1534/genetics.110.119917
927 Rewitz K F Y N, Gilbert L I , et al. (2009). The insect neuropeptide PTTH activates receptor
928 tyrosine kinase torso to initiate metamorphosis. *Science, 326*(5958), 1403-1405. doi:
929 10.1126/science.1176450

Rewitz K F, Yamanaka N, Gilbert L I, & O'Connor M B. (2009). The insect neuropeptide PTTH activates receptor tyrosine kinase torso to initiate metamorphosis. *Science, 326*(5958), 1403-1405. doi:10.1126/science.1176450

Rezával C, Nojima T, Neville M C, Lin A C, & Goodwin S F. (2014). Sexually dimorphic octopaminergic neurons modulate female postmating behaviors in Drosophila. *Curr Biol, 24*(7), 725-730. doi:10.1016/j.cub.2013.12.051

Rezával C, Pattnaik S, Pavlou H J, Nojima T, Brüggemeier B, D'Souza L A D, Dweck H K M, & Goodwin S F. (2016). Activation of latent courtship circuitry in the brain of Drosophila females induces male-like behaviors. *Curr Biol, 26*(18), 2508-2515. doi:10.1016/j.cub.2016.07.021

Riddiford L M, Cherbas P, & Truman J W. (2000). Ecdysone receptors and their biological actions. *Vitam Horm, 60*, 1-73. doi:10.1016/s0083-6729(00)60016-x

Rideout E J, Dornan A J, Neville M C, Eadie S, & Goodwin S F. (2010). Control of sexual differentiation and behavior by the doublesex gene in Drosophila melanogaster. *Nat Neurosci, 13*(4), 458-466. doi:10.1038/nn.2515

Roy S, Saha T T, Zou Z, & Raikhel A S. (2018). Regulatory pathways controlling female insect reproduction. *Annu Rev Entomol, 63*, 489-511. doi:10.1146/annurev-ento-020117-043258

Ruta V, Datta S R, Vasconcelos M L, Freeland J, Looger L L, & Axel R. (2010). A dimorphic pheromone circuit in Drosophila from sensory input to descending output. *Nature, 468*(7324), 686-690. doi:10.1038/nature09554

Scheffer L K, Xu C S, Januszewski M et al.. (2020). A connectome and analysis of the adult Drosophila central brain. *Elife, 9*. doi:10.7554/eLife.57443

Schretter C E, Aso Y, Robie A A, Dreher M, Dolan M J, Chen N, Ito M, Yang T, Parekh R, Branson K M, & Rubin G M. (2020). Cell types and neuronal circuitry underlying female aggression in Drosophila. *Elife, 9*. doi:10.7554/eLife.58942

Sengupta S, Chan Y B, Palavicino-Maggio C B, & Kravitz E A. (2022). GABA transmission from mAL interneurons regulates aggression in Drosophila males. *PNAS, 119*(5). doi:10.1073/pnas.2117101119

Shimell M, Pan X, Martin F A, Ghosh A C, Leopold P, O'Connor M B, & Romero N M. (2018). Prothoracicotropic hormone modulates environmental adaptive plasticity through the control of developmental timing. *Development, 145*(6). doi:10.1242/dev.159699

Siwicki K K, & Kravitz E A. (2009). Fruitless, doublesex and the genetics of social behavior in Drosophila melanogaster. *Curr Opin Neurobiol, 19*(2), 200-206. doi:10.1016/j.conb.2009.04.001

Stockinger P, Kvitsiani D, Rotkopf S, Tirián L, & Dickson B J. (2005). Neural circuitry that governs Drosophila male courtship behavior. *Cell, 121*(5), 795-807. doi:10.1016/j.cell.2005.04.026

Taisz I, Donà E, Münch D, Bailey S N, Morris B J, Meechan K I, Stevens K M, Varela-Martínez I, Gkantia M, Schlegel P, Ribeiro C, Jefferis G, & Galili D S. (2023). Generating parallel representations of position and identity in the olfactory system. *Cell, 186*(12), 2556-2573.e2522. doi:10.1016/j.cell.2023.04.038

Terhzaz S, Rosay P, Goodwin S F, & Veenstra J A. (2007). The neuropeptide SIFamide modulates sexual behavior in Drosophila. *Biochem Biophys Res Commun, 352*(2), 305-310. doi:10.1016/j.bbrc.2006.11.030

True, & John. (2014). Atlas of Drosophila Morphology: Wild-type and Classical Mutants. *Quarterly Review of Biology, 89*(2), 188-188.

Truman J W, & Riddiford L M. (2023). Drosophila postembryonic nervous system development: a model for the endocrine control of development. *Genetics, 223*(3). doi:10.1093/genetics/iyac184

Truman J W, Talbot W S, Fahrbach S E, & Hogness D S. (1994). Ecdysone receptor expression in the CNS correlates with stage-specific responses to ecdysteroids during Drosophila and Manduca development. *Development, 120*(1), 219-234. doi:10.1242/dev.120.1.219

von Philipsborn A C, Liu T, Yu J Y, Masser C, Bidaye S S, & Dickson B J. (2011). Neuronal control of Drosophila courtship song. *Neuron, 69*(3), 509-522. doi:10.1016/j.neuron.2011.01.011

Wang F, Wang K, Forknall N, Parekh R, & Dickson B J. (2020a). Circuit and Behavioral Mechanisms of sexual rejection by Drosophila females. *Curr Biol, 30*(19), 3749-3760 e3743. doi:10.1016/j.cub.2020.07.083

Wang F, Wang K, Forknall N, Patrick C, Yang T, Parekh R, Bock D, & Dickson B J. (2020b). Neural circuitry linking mating and egg laying in Drosophila females. *Nature, 579*(7797), 101-105. doi:10.1038/s41586-020-2055-9

Wang K, Wang F, Forknall N, Yang T, Patrick C, Parekh R, & Dickson B J. (2021). Neural circuit mechanisms of sexual receptivity in Drosophila females. *Nature, 589*(7843), 577-581. doi:10.1038/s41586-020-2972-7

Wang L, & Anderson D J. (2010). Identification of an aggression-promoting pheromone and its receptor neurons in Drosophila. *Nature, 463*(7278), 227-231. doi:10.1038/nature08678

Wang T, Jing B, Deng B, Shi K, Li J, Ma B, Wu F, & Zhou C. (2022). Drosulfakinin signaling modulates female sexual receptivity in Drosophila. *Elife, 11*. doi:10.7554/eLife.76025

Wu Y, Bidaye S, & Mahringer D. (2019). Drosophila female-specific brain neuron elicits persistent position- and direction-selective male-like social behaviors. doi:10.1101/594960

Yamamoto D. (2007). The neural and genetic substrates of sexual behavior in Drosophila. *Adv Genet, 59*, 39-66. doi:10.1016/S0065-2660(07)59002-4

Yamamoto D, & Koganezawa M. (2013). Genes and circuits of courtship behaviour in Drosophila males. *Nat Rev Neurosci, 14*(10), 681-692. doi:10.1038/nrn3567

Yamanaka N, Romero N M, Martin F A, Rewitz K F, Sun M, O'Connor M B, & Léopold P. (2013). Neuroendocrine control of Drosophila larval light preference. *Science, 341*(6150), 1113-1116. doi:10.1126/science.1241210

Yang C H, Rumpf S, Xiang Y, Gordon M D, Song W, Jan L Y, & Jan Y N. (2009). Control of the postmating behavioral switch in Drosophila females by internal sensory neurons. *Neuron, 61*(4), 519-526. doi:10.1016/j.neuron.2008.12.021

Zhou C, Pan Y, Robinett C C, Meissner G W, & Baker B S. (2014). Central brain neurons expressing doublesex regulate female receptivity in Drosophila. *Neuron, 83*(1), 149-163. doi:10.1016/j.neuron.2014.05.038

1016 **Figure Legends**

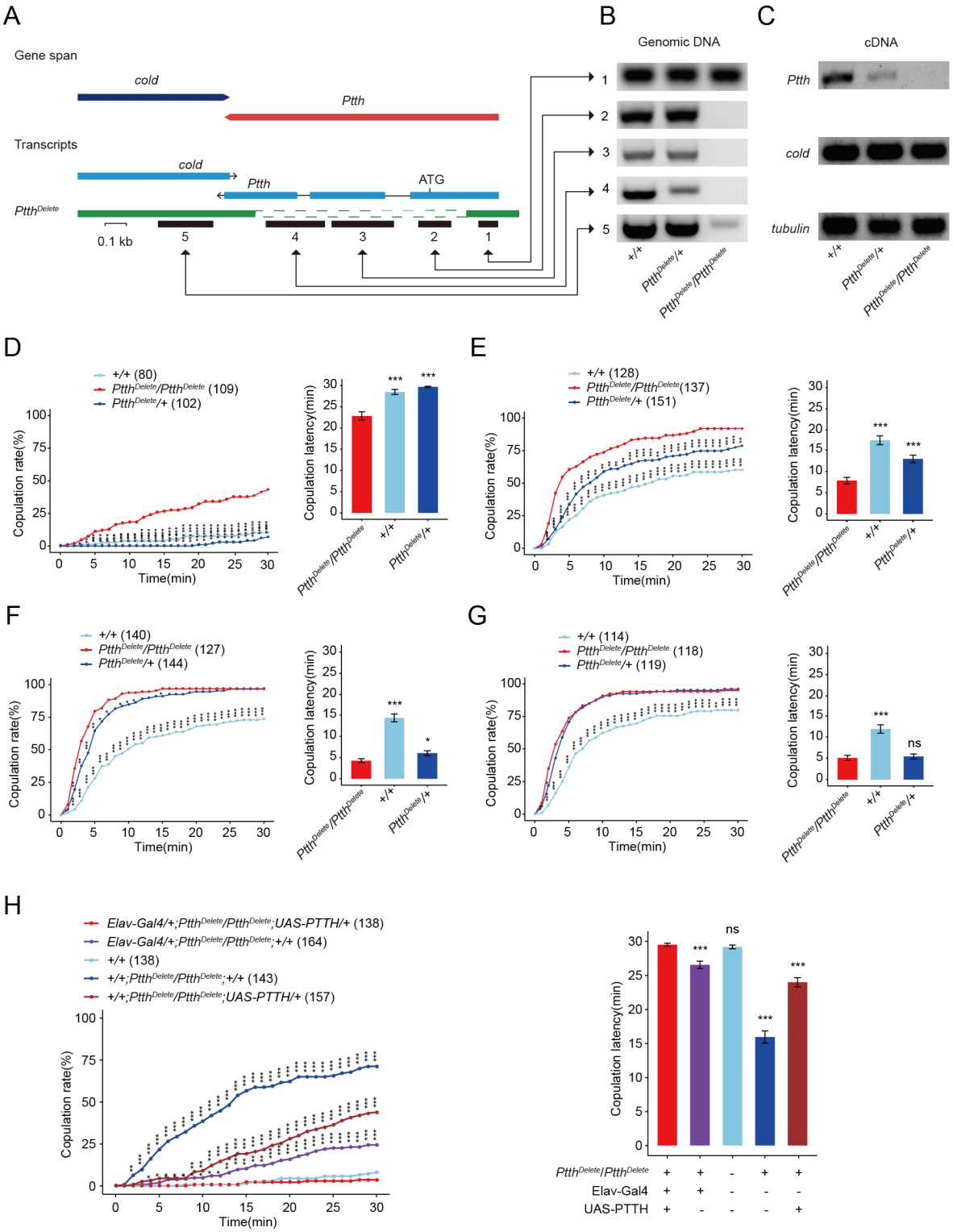

1017

1018 **Figure 1 *Ptth* null mutants have increased virgin female receptivity.**

1019 (A-C) Generation and validation of a 974 bp deletion mutant of the *Ptth* gene. The 5'
1020 UTR and almost all coding sequence were deleted. The deletion was confirmed through
1021 PCR analysis at the PTTH locus in genomic DNA samples (B), and through RT-PCR to
1022 identify the loss of PTTH transcripts in cDNA samples of wandering larvae (C). (D-G)
1023 Virgin female receptivity of *Ptth* null mutants on the 1st (D), 2nd (E), 3rd (F) and 6th day
1024 (G) respectively. The comparison referred to $Ptth^{Delete}/Ptth^{Delete}$. (H) Enhanced virgin
1025 female receptivity of *ΔPtth* null mutants was rescued by elav-Gal4 driving UAS-PTTH.
1026 The increased copulation rate and decreased latency to copulation on the 1st day after
1027 eclosion were rescued to the comparable level of control. The comparison referred to
1028 *elav-Gal4/+;* $Ptth^{Delete}/Ptth^{Delete}$*;UAS-PTTH/+*. The copulation latency *and copulation rate*
1029 of *elav-Gal4/+;* $Ptth^{Delete}/Ptth^{Delete}$ is higher and lower than $Ptth^{Delete}/Ptth^{Delete}$*;UAS-*
1030 *PTTH/+ respectively*. The number of female flies paired with wild type males is
1031 displayed in parentheses. For the copulation rate, chi-square test is applied. For the
1032 latency to copulation, Kruskal-Wallis ANOVA and post hoc Mann-Whitney U tests are
1033 applied. Error bars indicate SEM. *$p < 0.05$, **$p < 0.01$, ***$p < 0.001$, ****$p < 0.0001$, ns
1034 indicates no significant difference.
1035
1036
1037
1038
1039
1040
1041
1042
1043
1044
1045
1046

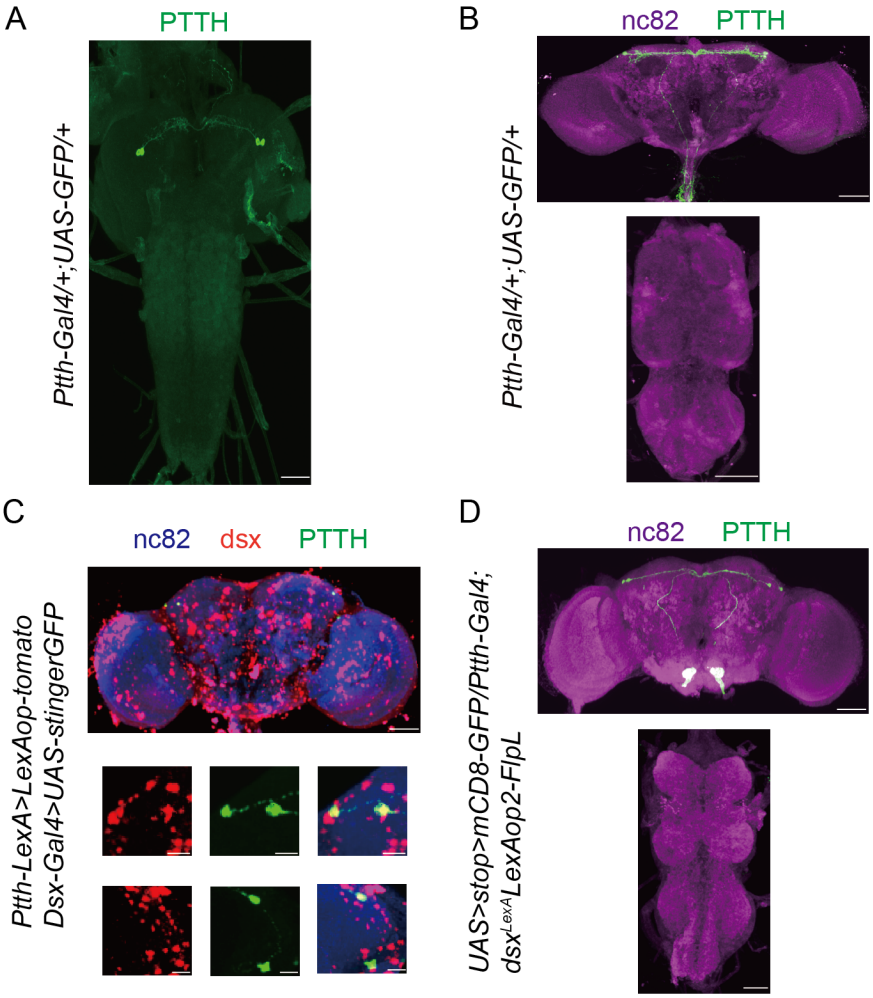

Figure 2 PTTH neurons are doublesex-positive neurons.

(A-B) Expression pattern of Ptth-Gal4 revealed by anti-GFP in larvae central nervous system (CNS) (A) and adult brain (B). Representative of five female flies. Scale bars, 50 μm. (C) All PTTH neurons were colabeled by dsx-Gal4 driving UAS-GFP-Stinger (red) and Ptth-LexA driving LexAop-tomato (green). Representative of five female brains. Scale bars, 50 μm and 5 μm (zoom-in). (D) All PTTH neurons were *Ptth* and *Dsx* co-expressing, labeled by intersectional strategy. The larvae flies were the wandering ones. The adult flies were within-10 hours-old adults. Representative of 5 female brains. Scale bars, 50 μm.

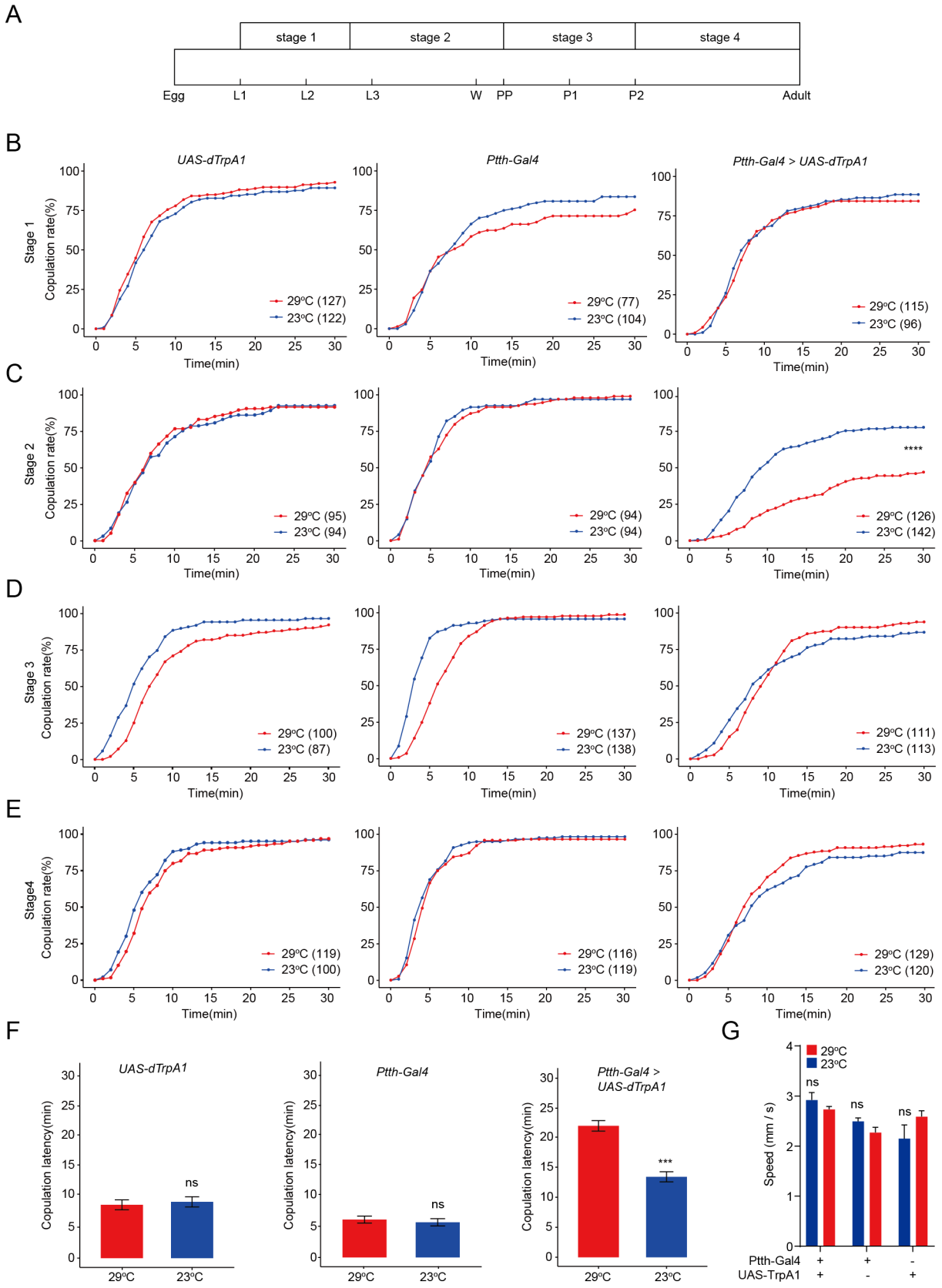
A
stage 1
stage 2
stage 3
stage 4
Egg
L1
L2
L3
W
PP
P1
P2
Adult
B
UAS-dTrpA1
Ptth-Gal4
Ptth-Gal4 > UAS-dTrpA1
Stage 1
Copulation rate(%)
Time(min)
29ºC (127)
23ºC (122)
29ºC (77)
23ºC (104)
29ºC (115)
23ºC (96)
C
Stage 2
29ºC (95)
23ºC (94)
29ºC (94)
23ºC (94)
****
29ºC (126)
23ºC (142)
D
Stage 3
29ºC (100)
23ºC (87)
29ºC (137)
23ºC (138)
29ºC (111)
23ºC (113)
E
Stage4
29ºC (119)
23ºC (100)
29ºC (116)
23ºC (119)
29ºC (129)
23ºC (120)
F
Copulation latency(min)
ns
***
29ºC
23ºC
G
Speed (mm / s)
Ptth-Gal4
UAS-TrpA1

1058

1059

1060 **Figure 3 Activation of PTTH neurons expressing PTTH during the 3rd-instar larvae**
1061 **inhibits virgin female receptivity.**
1062 (A) Four developmental stages of *Drosophila* before eclosion when PTTH neurons were
1063 thermogenetic activated by dTrpA1. L1, L2, and L3: start of three larval stages, W: start
1064 of wandering stage, Pp: puparium formation, P1 and P2: start of the 1st and 2nd day of
1065 pupal stage. (B-E) Ptth-Gal4 driving UAS-dTrpA1 activated PTTH neurons at 29°C.
1066 Activation of PTTH neurons at the stage 2 significantly decreased copulation rate (C),
1067 but not at the stage 1 (B), stage 3 (D) and stage 4 (E). (F) Activation of PTTH neurons
1068 at the stage 2 significantly increased the latency to copulation. (G) Mean velocity had no
1069 significant change when PTTH neurons were activated during the stage 2 compared
1070 with control females (ns = not significant, Kruskal-Wallis ANOVA and post hoc Mann-
1071 Whitney U tests, mean ± SEM, n = 8-12). The comparison referred to *Ptth-Gal4/UAS-*
1072 *dTrpA1*. Female flies were 4-days-old adults. The number of female flies paired with
1073 wild-type males is displayed in parentheses. For the copulation rate, chi-square test is
1074 applied. For the latency to copulation, Mann-Whitney U test is applied. Error bars
1075 indicate SEM. *$p < 0.05$, **$p < 0.01$, ***$p < 0.001$, ****$p < 0.0001$, ns indicates no
1076 significant difference.
1077
1078
1079
1080
1081
1082
1083
1084
1085
1086
1087
1088
1089

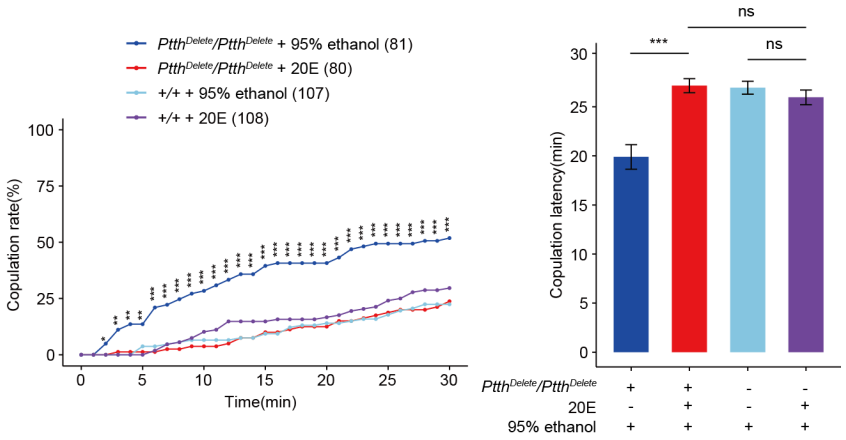

Figure 4 Feeding 20E restores virgin female receptivity of *Ptth* null mutant flies. (A-B) The increased copulation rate and decreased latency to copulation of the 24h-old *ΔPtth* flies were rescued to the comparable level of wild type females by feeding 20E to the 3rd-instar larval *ΔPtth* flies. The wild type larval females fed by 20E had no significantly different copulation rate and latency to copulation compared with the wild type females fed by the same volume of 95% ethanol which is the solvent of 20E. The comparison referred to *Ptth*^{Delete}/*Ptth*^{Delete} + 20E. Female flies were 1-day-old. The number of female flies paired with wild-type males is displayed in parentheses. For the copulation rate, chi-square test is applied. For the latency to copulation, Kruskal-Wallis ANOVA and post hoc Mann-Whitney U tests are applied. Error bars indicate SEM. *$p < 0.05$, **$p < 0.01$, ***$p < 0.001$, ****$p < 0.0001$, ns indicates no significant difference.

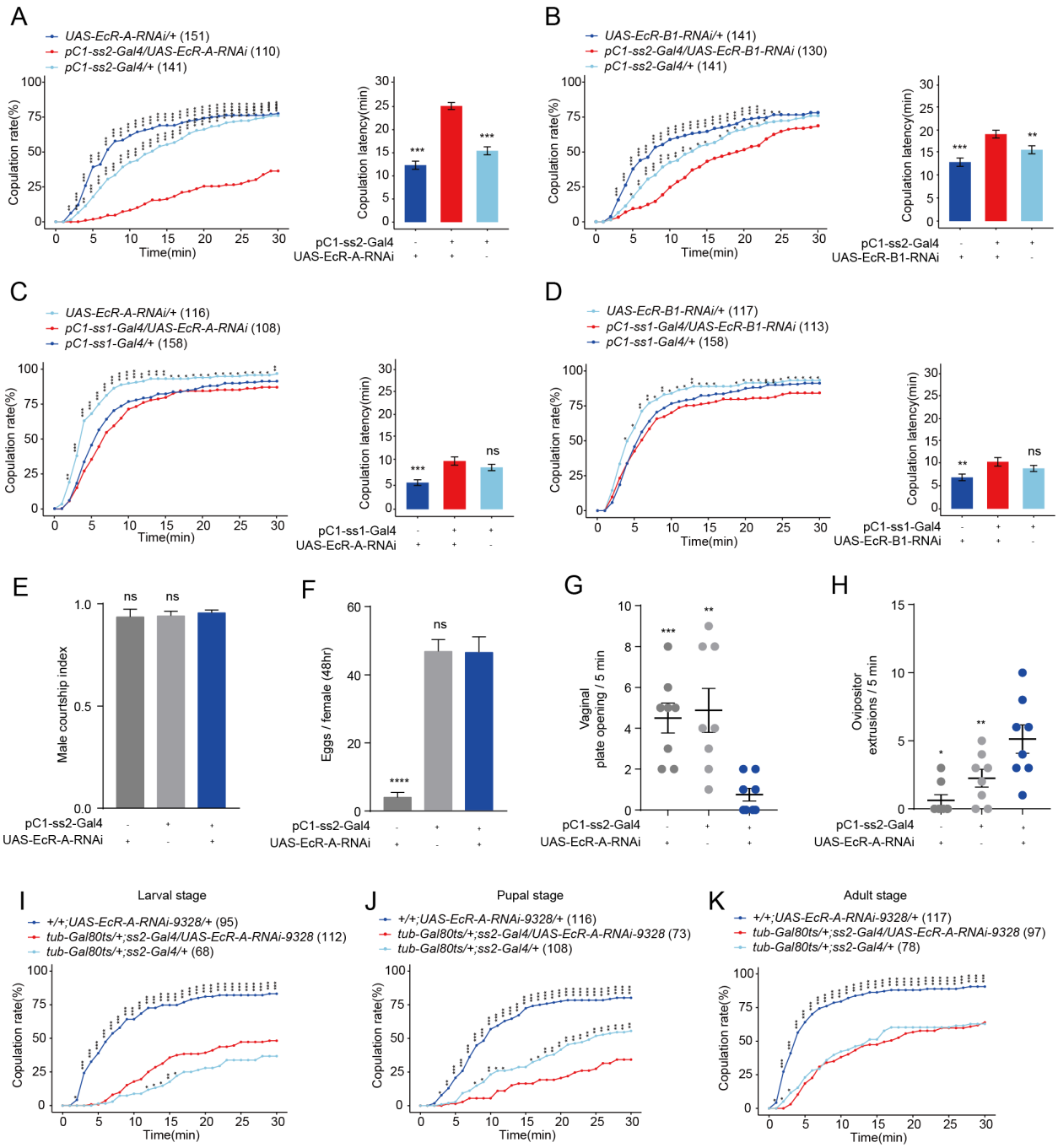

Figure 5 Virgin females with reduced EcR-A in pC1 neurons have reduced sexual receptivity.

(A) Knock-down of EcR-A in pC1 neurons driven by pC1-ss2-Gal4 significantly decreased the copulation rate and increased the latency to copulation. (B) Knock-down of EcR-B1 in pC1 neurons driven by pC1-ss2-Gal4 significantly prolonged the latency to copulation. (C-D) Knock-down of EcR-A (C) or EcR-B1 (D) in pC1 neurons driven by

1121 pC1-ss1-Gal4 did not affect the copulation rate or the latency to copulation. (E)
1122 Courtship index of wild-type males towards a female with the indicated genotype (n =
1123 8). (F) The number of eggs laid by virgin females during the 3rd - 4th day after eclosion
1124 when EcR-A was knocked down in pC1 neurons (n = 17-36). The UAS-EcR-A-RNAi
1125 control causes a massive decrease in female fertility. (G) Knock-down of EcR-A in pC1
1126 neurons decreased the opening of vaginal plate of virgin females compared with
1127 controls (n = 8). (H) Knock-down of EcR-A in pC1 neurons increased the ovipositor
1128 extrusion of virgin females compared with controls (n = 8). (I-K) Virgin female copulation
1129 rate when EcR-A was knocked down in pC1 neurons temporally restricted by shifts from
1130 18°C to 30°C. EcR-A was knocked down during the whole larval (I), pupal (J) and adult
1131 (K) stages respectively. When the experiment was done at the pupal stage is the only
1132 situation when the controls were both different from the experimental (J). The
1133 comparison referred to flies with decreased EcR isoform in pC1 neurons. Female flies
1134 for behavioral assay were 4-6-days-old adults. The number of female flies paired with
1135 wild-type males is displayed in parentheses. For the copulation rate, chi-square test is
1136 applied. For other comparisons, Kruskal-Wallis ANOVA and post hoc Mann-Whitney U
1137 tests are applied. Error bars indicate SEM. *$p < 0.05$, **$p < 0.01$, ***$p < 0.001$, ****$p <$
1138 0.0001, ns indicates no significant difference.
1139
1140
1141
1142
1143
1144
1145
1146
1147
1148
1149
1150

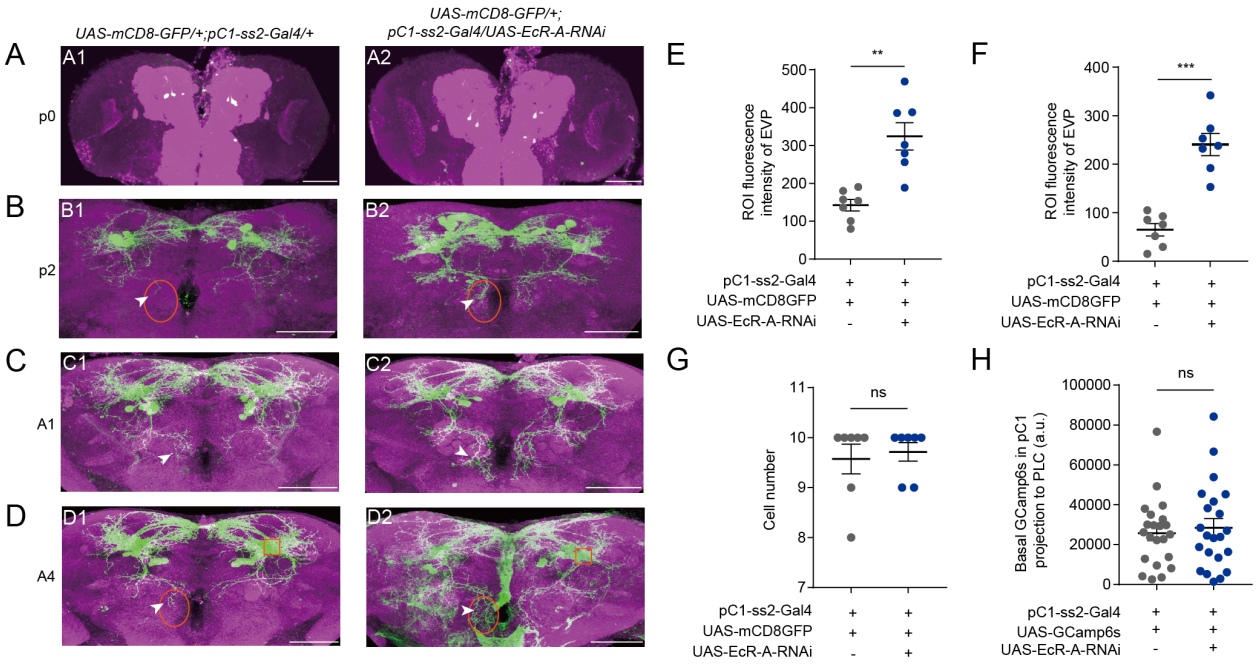

Figure 6 Reduced EcR-A in pC1 neurons induces the morphological changes. (A1-A2) pC1-ss2-Gal4 expressing neurons appeared at the start of the pupal stage. (B-D) Reduced EcR-A in pC1 neurons induced more elaborated morphologies of pC1d axons, especially the extra vertical projection (EVP). The EVP regions of pC1d neurons was indicated by arrows. The morphological changes appeared on the 2nd day of the pupal stage (B1-B2) and retained to the adult stage including the 1st day (C1-C2) and the 4th day (D1-D2) of the adult stage. p0, the 1st day of the pupal stage; p2, the 2nd day of the pupal stage; A1, the 1st day of the adult stage; A4, the 4th day of the adult stage. (E-F) Fluorescence intensity of EVP in pC1d neurons on the 2nd day of the pupal stage (E) and the 4th day of the adult stage (F) was quantified when EcR-A was reduced in pC1 neurons (n=7). The quantified EVP regions were marked in (B) and (D) with orange ellipses. (G) pC1 neurons of the 4th day adults had comparable cell body number when EcR-A was reduced in pC1 neurons or not (n = 7). (H) Basal GCaMP6s signals in the LPC region of pC1 neurons when EcR-A was reduced in pC1 neurons (n = 22). LPC regions, the neurites extending from pC1 cell bodies, were marked with orange square in (D1) and (D2). The comparison referred to flies with decreased EcR isoform in pC1 neurons. Female flies in (G-H) were 4-days-old adults. Scale bars are 50 μm. For all comparisons, Mann-Whitney U test is applied. Error bars indicate SEM. *$p < 0.05$, **$p < 0.01$, ***$p < 0.001$, ****$p < 0.0001$, ns indicates no significant difference.

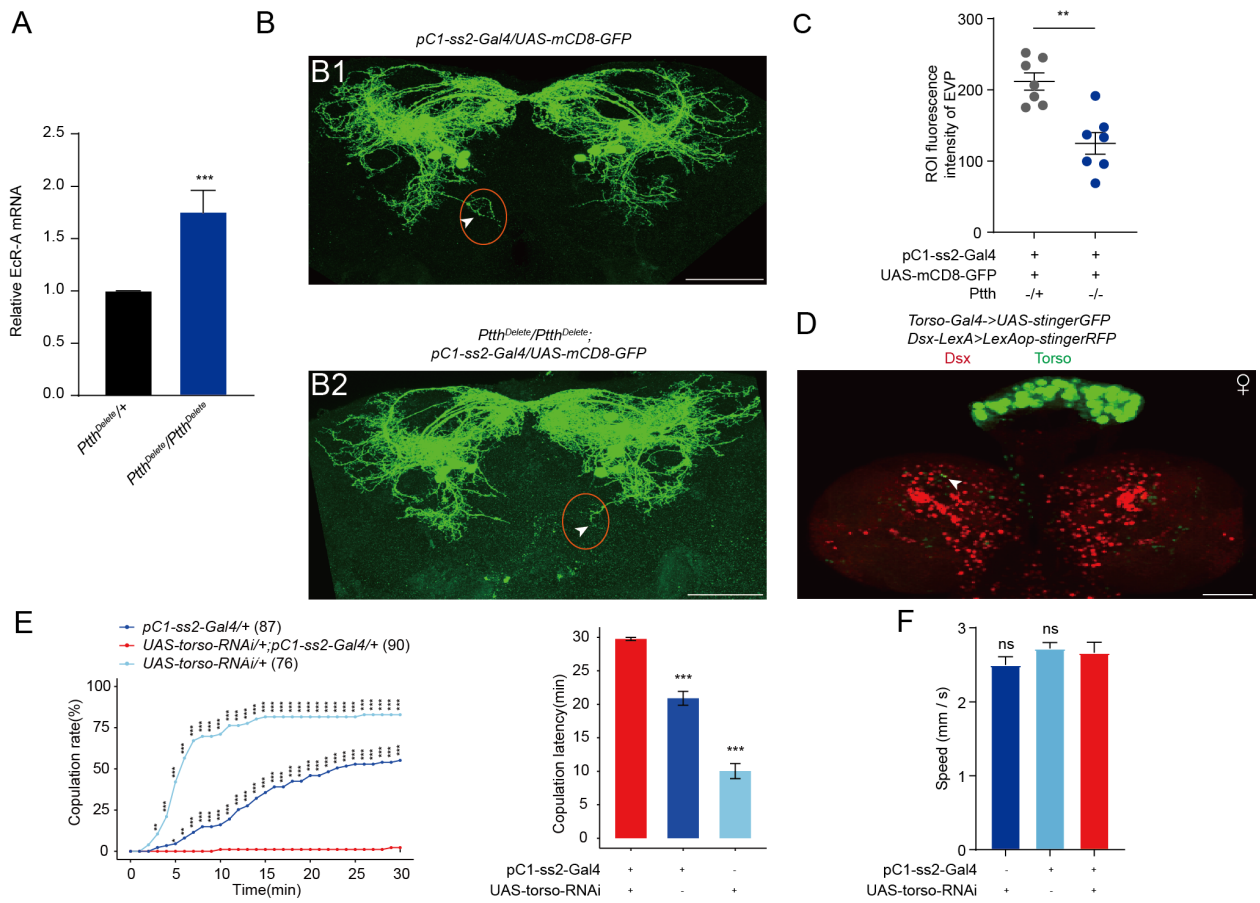

Figure 7 The function of PTTH on EcR-A and pC1 neurons.

(A) qRT-PCR for EcR-A when PTTH was deleted. Bars represent mean ± SEM. p values are from Mann-Whitney U test (n = 8 for *Ptth*^{Delete}/+ and n = 6 for *Ptth*^{Delete}/*Ptth*^{Delete}, each sample contains about 10 bodies of newly formed prepupae). *p < 0.05, **p < 0.01, ***p < 0.001, ****p < 0.0001, ns indicates no significant difference. (B) Deletion of PTTH induced less elaborated morphologies of pC1d axons, especially the extra vertical projection (EVP). The EVP regions of pC1d neurons was indicated by arrows. Female flies were 4-days-old adults. (C) Fluorescence intensity of EVP in pC1d neurons on the 4th day was quantified when PTTH was deleted (n=7). The quantified EVP regions were marked in (B1) and (B2) with red ellipses. (D) Torso-Gal4 and Dsx-LexA were labeled by stinger GFP and stingerRFP respectively. Arrows indicated the overlap of GFP and RFP signals. Representative of five female brains. Scale bars, 50 μm. (E-F) Knock-down of Torso in pC1 neurons inhibited virgin female copulation rate and enhanced latency to copulation. Females had similar locomotion speeds between

1186 groups (F). The pC1-ss2-Gal4 control causes a massive decrease in female receptivity.
1187 The comparison referred to pC1-ss2-Gal4/UAS-torso-RNAi. Female flies were 4-6-days-
1188 old adults. The number of female flies paired with wild-type males is displayed in
1189 parentheses. For the copulation rate, chi-square test is applied. For the latency to
1190 copulation, Kruskal-Wallis ANOVA and post hoc Mann-Whitney U tests are applied.
1191 Error bars indicate SEM, *$p < 0.05$, **$p < 0.01$, ***$p < 0.001$, ****$p < 0.0001$, ns indicates
1192 no significant difference.
1193
1194
1195
1196
1197
1198
1199
1200
1201
1202
1203
1204
1205
1206
1207
1208
1209
1210
1211
1212
1213
1214
1215
1216

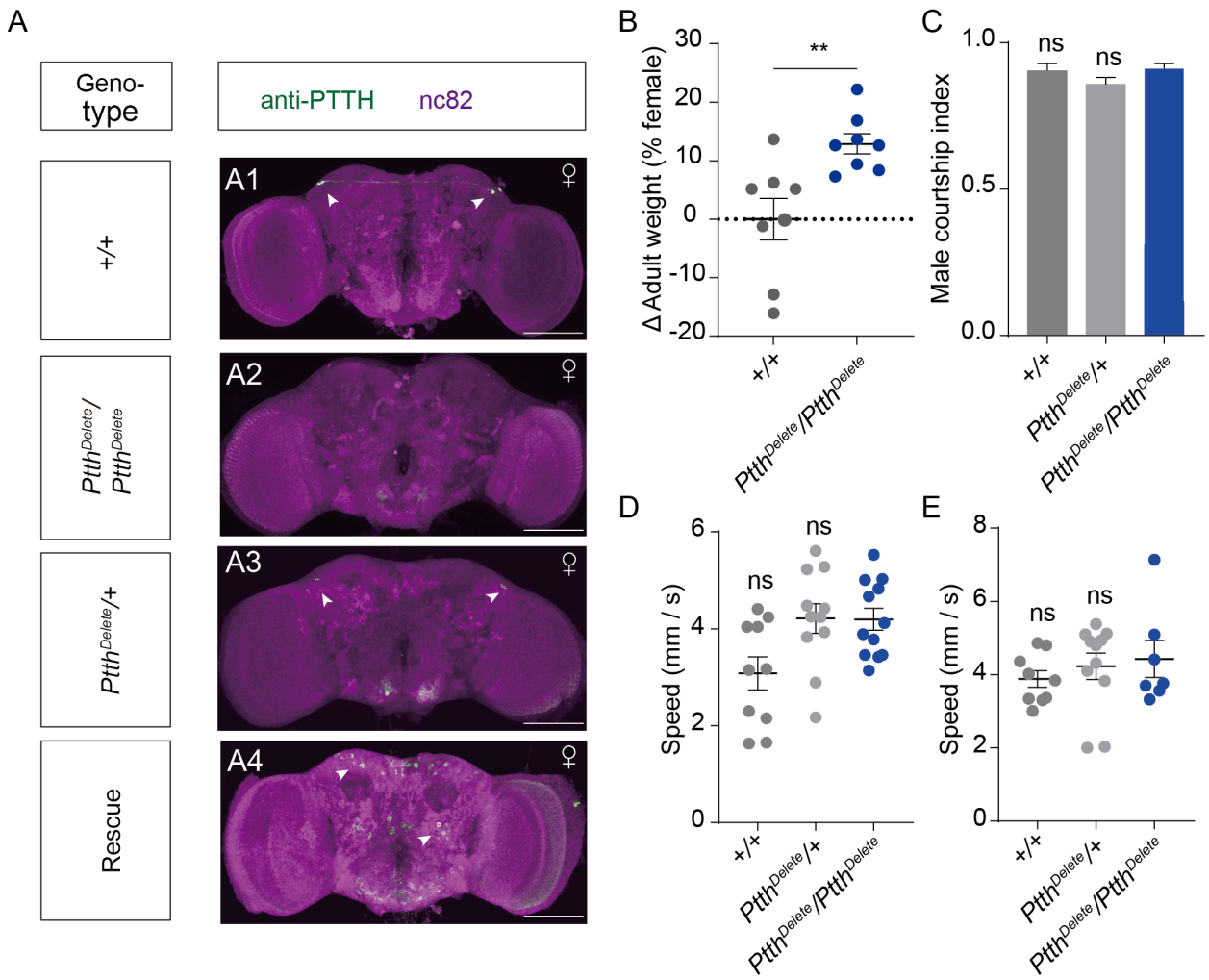

Figure 1—figure supplement 1 PTTH expression, weight, attractiveness and locomotion behavior of *Ptth* null mutant virgin females.

(A) Brain of indicated genotype, immunostained with anti-PTTH antibody (green) and counterstained with nc82 (magenta). Arrows show signals (green) stained with anti-PTTH antibody. Female flies were within 10 hours after eclosion. Scale bars, 50 μm. (B) The weights of 24h-old adult $Ptth^{Delete}/Ptth^{Delete}$ null mutant females were significantly higher than that of wild type females (Mann-Whitney U test, n=8 groups, 10 flies in each group). (C) Courtship index of wild-type males during the first 5 min of courtship towards a female with the indicated genotype (Kruskal-Wallis ANOVA and post hoc Mann-Whitney U tests, n = 7-9). (D-E) Mean velocity had no significant change in $Ptth^{Delete}/Ptth^{Delete}$ null mutant females on the 1st day (D) and the 6th day (E) compared with control females (Kruskal-Wallis ANOVA and post hoc Mann-Whitney U tests, n = 7-

12). The comparison referred to *Ptth*^{Delete}/*Ptth*^{Delete}. Female flies for behavioral assay were 4-6-days-old adults. Error bars indicate SEM. *p < 0.05, **p < 0.01, ***p < 0.001, ****p < 0.0001, ns = not significant.

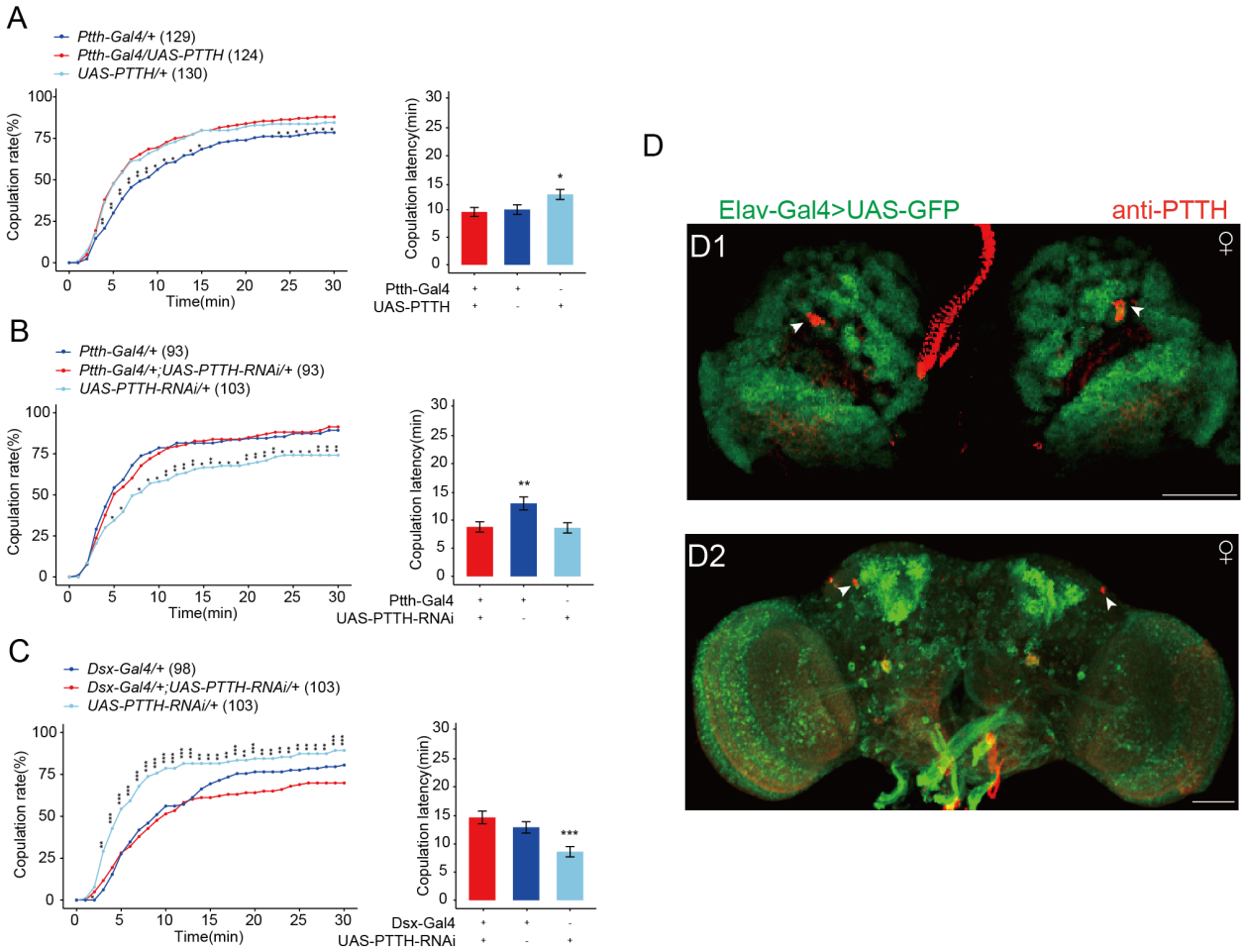

Figure 1—figure supplement 2 Effect of the expression of PTTH on female receptivity.

(A) Overexpressing PTTH in PTTH neurons. The comparison referred to flies *Ptth-Gal4/+;UAS-PTTH/+.* Female flies for behavioral assay were 4-6 days-old. (B-C) Decreasing PTTH in PTTH neurons. The comparison referred to flies *Ptth-Gal4/+;UAS-PTTH-RNAi/+* and *Dsx-Gal4/+;UAS-PTTH-RNAi/+.* Female flies for behavioral assay were 2-days-old adults. (D) The fly brain of elav-Gal4>UAS-GFP were stained with PTTH antibody. The larvae flies were the wandering ones. The adult flies were within 10 hours after eclosion. Representative of 5 female brains. Scale bars, 50 μm.

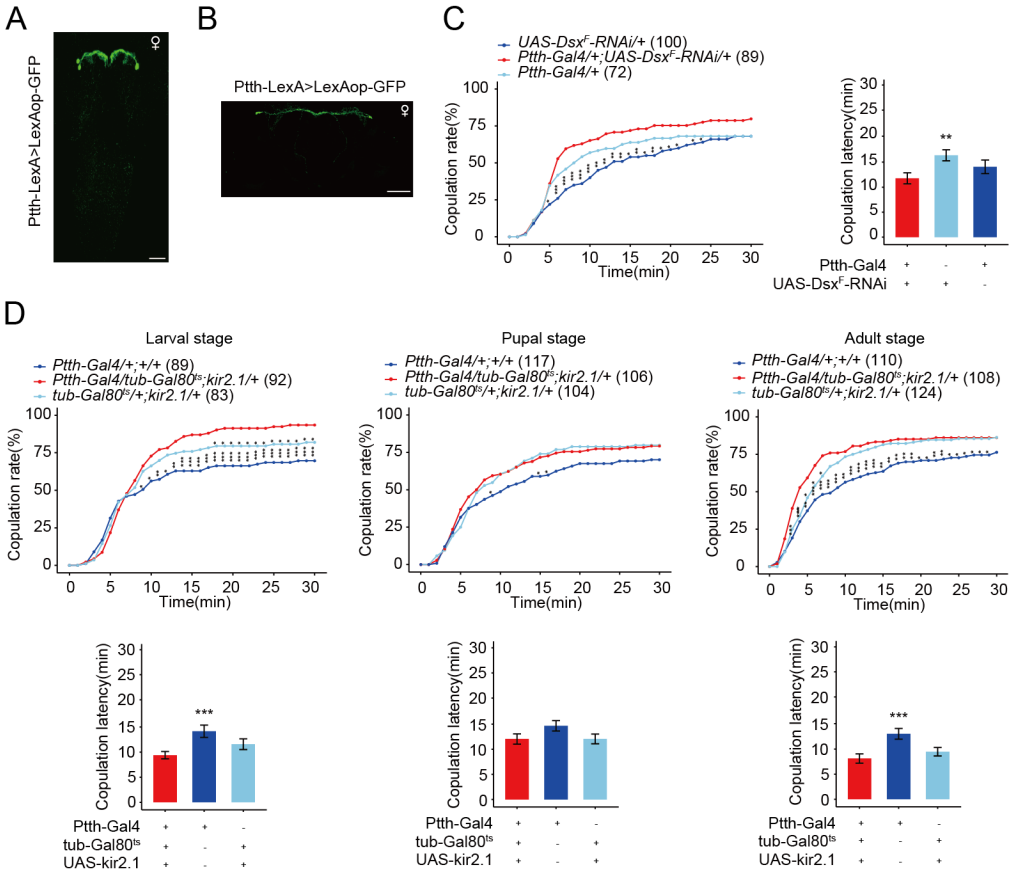

Figure 2—figure supplement 1 The function of PTTH neurons in female receptivity.

Expression pattern of Ptth-LexA in the brain revealed by anti-GFP (green) in wandering larvae CNS (A) and within-10-hours adult brain (B). Representative of five female flies. Scale bars, 50 μm. (C) The female receptivity when deceasing the expression of Dsx^F in PTTH neurons. The comparison referred to *Ptth-Gal4/+;UAS-Dsx^F-RNAi/+*. Female flies were 2-days-old adults. (D) PTTH neurons were inactivated during the whole larval, pupal and adult stages respectively by kir2.1, restricted by shifts from 18°C to 30°C. When the experiment was done at the larval stage is the only situation when the controls were both different from the experimental. The comparison referred to *Ptth-Gal4/tub-Gal80ts;kir2.1/+*. Female flies were 2-days-old adults. The number of female flies paired with wild-type males is displayed in parentheses. For the copulation rate, chi-square test is applied. Error bars indicate SEM. *$p < 0.05$, **$p < 0.01$, ***$p < 0.001$, ****$p < 0.0001$, ns indicates no significant difference.

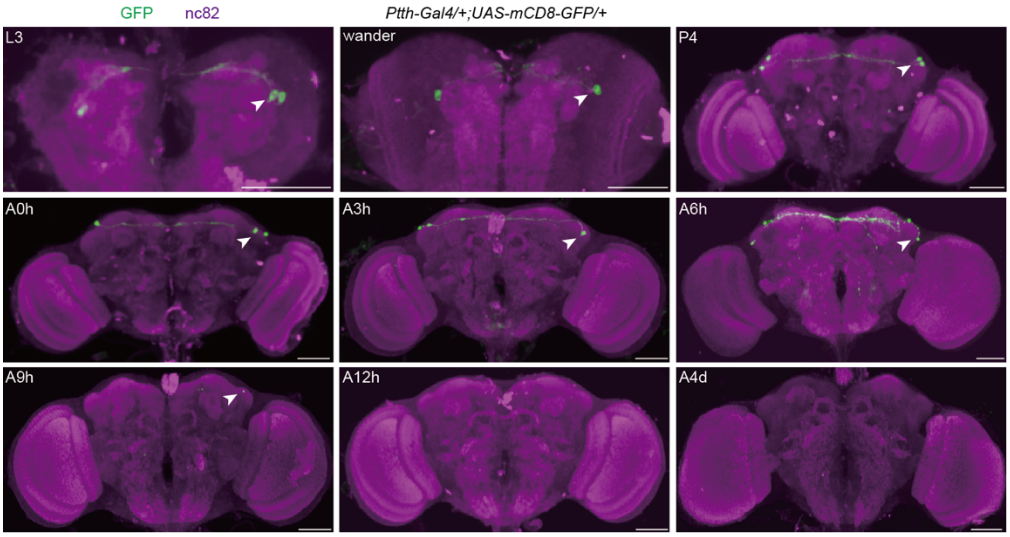

Figure 2—figure supplement 2 The anatomical pattern of PTTH neurons expressing PTTH at different developmental stages.

Expression pattern of Ptth-Gal4 in the brain revealed by anti-GFP from the 3rd larval stage to the 4th day after eclosion. Arrows show PTTH signals (green) stained with anti-GFP antibody. L3, the 3rd -instar larvae; wander, the wandering larvae; P4, the 4th day of the pupal stage; A0h, the 1st hour of the adult stage; A3h, the 3rd hour of the adult stage; A6h, the 6th hour of the adult stage; A9h, the 9th hour of the adult stage; A12h, the 12th hour of the adult stage; A4d, the 4th day of the adult stage. Representative of five female flies. Scale bars, 50 μm.

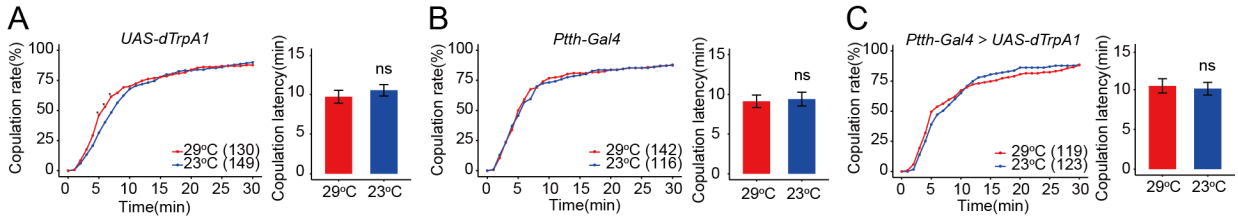

Figure 2—figure supplement 3 PTTH neurons expressing PTTH do not regulate virgin female copulation rate during adult stage.

PTTH neurons were activated during adult stage by dTrpA1 at 29°C. The female copulation rate and the latency to copulation did not change significantly. The number of female flies paired with wild-type males is displayed in parentheses. Female flies were 4-days-old adults. For the copulation rate, chi-square test is applied. For the latency to copulation, Mann-Whitney U test is applied. Error bars indicate SEM. *$p < 0.05$, **$p < 0.01$, ***$p < 0.001$, ****$p < 0.0001$, ns indicates no significant difference.

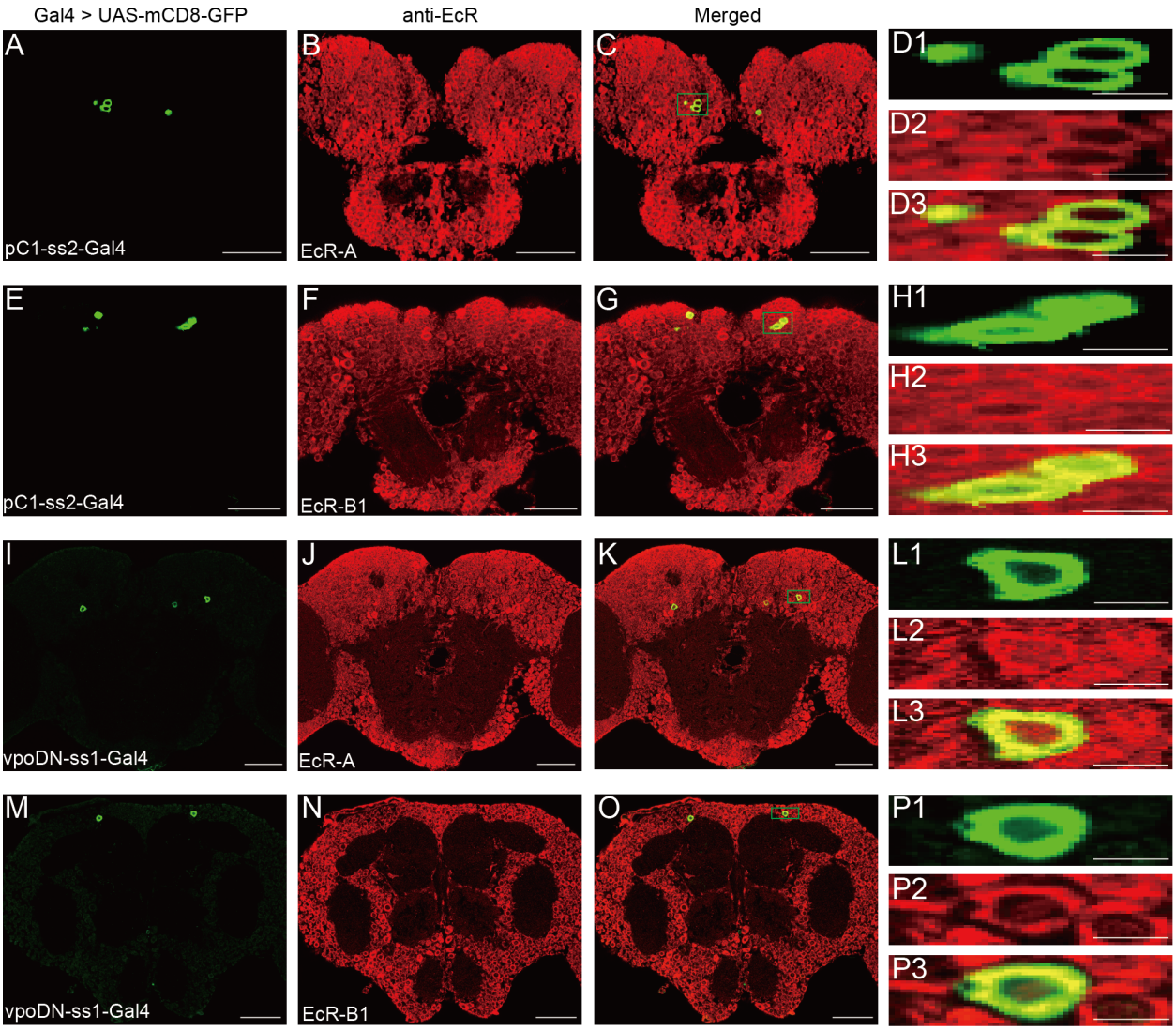

Figure 5—figure supplement 1 Expression of EcR-A and EcR-B1 in pC1 and vpoDN neurons.

(A-C) pC1 neurons were colabeled by pC1-ss2 driving UAS-mCD8-GFP (green, A) and EcR-A antibodies (red, B). Magnification of green boxed region in (C) is shown in (D1–D3). (E-G) pC1 neurons were colabeled by pC1-ss2 driving UAS-mCD8-GFP (green, E) and EcR-B1 antibodies (red, F). Magnification of green boxed region in (G) is shown in (H1–H3). (I-K) vpoDN neurons were colabeled by vpo-ss1 driving UAS-mCD8-GFP (green, I) and EcR-A antibodies (red, J). Magnification of green boxed region in (K) is shown in (L1–L3). (M-O) vpoDN neurons were colabeled by vpo-ss1 driving UAS-mCD8-GFP (green, M) and EcR-B1 antibodies (red, N). Magnification of green boxed

1347 region in (O) is shown in (P1–P3). Female flies were during prepupae stage. Scale bars
1348 for magnified regions are 5 μm, for others are 50 μm.
1349
1350
1351
1352
1353
1354
1355
1356
1357
1358
1359
1360
1361
1362
1363
1364
1365
1366
1367
1368
1369
1370
1371
1372
1373
1374
1375
1376
1377

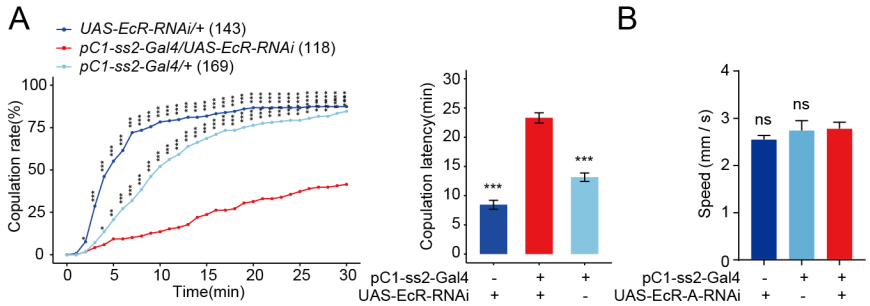

Figure 5—figure supplement 2 Reduced EcR in pC1 neurons reduces virgin female receptivity.

(A) Knock-down of EcR in pC1 neurons driven by pC1-ss2-Gal4 significantly decreased the copulation rate and increased the latency to copulation. (B) Mean velocity had no significant change when EcR-A was knocked down in pC1 neurons compared with controls (Kruskal-Wallis ANOVA and post hoc Mann-Whitney U tests, n = 8-11). The comparison referred to pC1-ss2-Gal4/UAS-EcR-RNAi (A) and pC1-ss2-Gal4/UAS-EcR-A-RNAi (B). Female flies were 4-6-days-old adults. The number of female flies paired with wild-type males is displayed in parentheses. For the copulation rate, chi-square test is applied. For the latency to copulation, Kruskal-Wallis ANOVA and post hoc Mann-Whitney U tests are applied. Error bars indicate SEM. *p < 0.05, **p < 0.01, ***p < 0.001, ****p < 0.0001, ns indicates no significant difference.

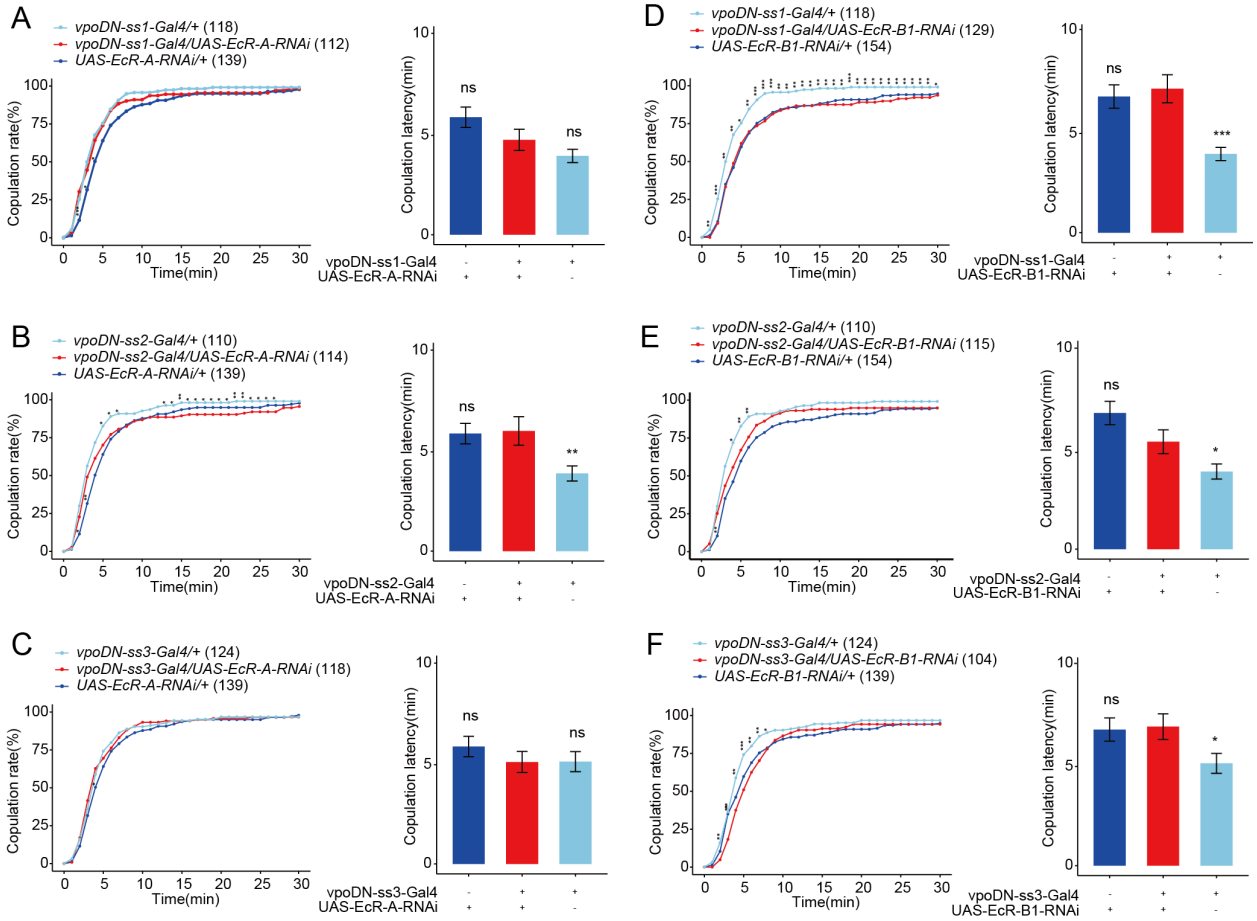

Figure 5—figure supplement 3 Reduced EcR in vpoDN neurons has no effect on virgin female receptivity.

(A-C) Knock-down of EcR-A in vpoDN neurons driven by vpoDN-ss1-Gal4, vpoDN-ss2-Gal4 and vpoDN-ss3-Gal4 had no effect on virgin female receptivity. (D-F) Knock-down of EcR-B1 in vpoDN neurons driven by vpoDN-ss1-Gal4, vpoDN-ss2-Gal4 and vpoDN-ss3-Gal4 had no effect on virgin female receptivity. The comparison referred to flies with decreased EcR isoform in vpoDN neurons. Female flies were 4-6-days-old adults. The number of female flies paired with wild-type males is displayed in parentheses. For the copulation rate, chi-square test is applied. For the latency to copulation, Kruskal-Wallis ANOVA and post hoc Mann-Whitney U tests are applied. Error bars indicate SEM. *$p < 0.05$, **$p < 0.01$, ***$p < 0.001$, ****$p < 0.0001$, ns indicates no significant difference.

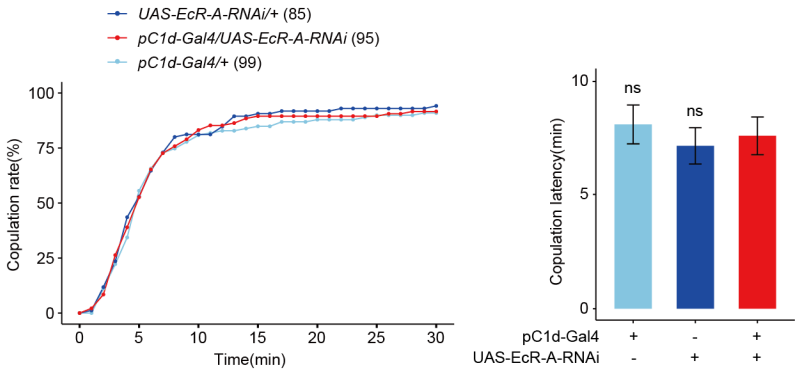

Figure 5—figure supplement 4 Reduced EcR-A in pC1d neurons has no effect on virgin female receptivity.

(A) Knock-down of EcR-A in pC1d neurons had no effect on virgin female copulation rate and latency to copulation. The comparison referred to pC1d-Gal4/UAS-EcR-A-RNAi. Female flies were 4-6-days-old adults. The number of female flies paired with wild-type males is displayed in parentheses. For the copulation rate, chi-square test is applied. For the latency to copulation, Kruskal-Wallis ANOVA and post hoc Mann-Whitney U tests are applied. Error bars indicate SEM, *p < 0.05, **p < 0.01, ***p < 0.001, ****p < 0.0001, ns indicates no significant difference.

1444 **Supplementary File 1.** The primers used for the verification of *Ptth*^{Delete} null mutant flies
1445 and for the real-time quantitative PCR of EcR-A when PTTH is deleted.
1446
1447 **Figure 1—Source Data 1.** Photo of nucleic acid electrophoresis and copulation time.
1448
1449 **Figure 2—Source Data 1.** Copulation time.
1450
1451 **Figure 3—Source Data 1.** Copulation time and walking speed.
1452
1453 **Figure 4—Source Data 1.** Copulation time.
1454
1455 **Figure 5—Source Data 1.** Copulation time, courtship index, number of eggs, number of
1456 vaginal plate opening (VPO), and number of ovipositor extrusion (OE).
1457
1458 **Figure 6—Source Data 1.** Fluorescence intensity, cell number and calcium activity.
1459
1460 **Figure 7—Source Data 1.** Relative mRNA level, fluorescence intensity, copulation time
1461 and walking speed.
1462
1463 **Figure 1—figure supplement 1—Source Data 1.** Body weight, courtship index and
1464 walking speed.
1465
1466 **Figure 1—figure supplement 2—Source Data 1.** Copulation time.
1467
1468 **Figure 2—figure supplement 1—Source Data 1.** Copulation time.
1469
1470 **Figure 2—figure supplement 3—Source Data 1.** Copulation time.
1471
1472 **Figure 5—figure supplement 2—Source Data 1.** Copulation time and walking speed.
1473
1474 **Figure 5—figure supplement 3—Source Data 1.** Copulation time.

1475

1476 **Figure 5—figure supplement 4—Source Data 1.** Copulation time.

1477